Available online at www.sciencedirect.com
ScienceDirect
Journal of Catalysis 243 (2006) 108–130
JOURNAL OF CATALYSIS
www.elsevier.com/locate/jcat

Solvent effects in liquid-phase reactions I. Activity and selectivity during citral hydrogenation on Pt/SiO_2 and evaluation of mass transfer effects

Samrat Mukherjee [1], M. Albert Vannice *

Department of Chemical Engineering, Pennsylvania State University, University Park, PA 16802-4400, USA

Received 28 April 2006; revised 19 June 2006; accepted 22 June 2006

Available online 23 August 2006

Abstract

The effect of the solvent on the liquid-phase hydrogenation of citral on a Pt/SiO_2 catalyst was examined by comparing the specific activity and the product selectivity in eight nonreactive solvents—*n*-amyl acetate, ethyl acetate, *n*-hexane, cyclohexane, tetrahydrofuran, *p*-dioxane, ethanol, and cyclohexanol—that have significantly different physical and electronic properties. Appendix A describes a detailed approach to calculating the properties of complex molecules that are required to determine an accurate Weisz–Prater criterion (or a Thiele modulus) to evaluate the presence or absence of pore diffusion limitations. These properties include viscosity, heat of vaporization, specific volume, and gas solubility in pure liquids or mixtures. Their utilization to calculate accurate effective diffusivities in porous catalysts is presented. All rate data utilized here were obtained in the kinetic regime. The absence of Cl in the catalyst prevented side reactions producing acetals. In a regime of kinetic control between 298 and 423 K, the turnover frequency (TOF) varied by a factor of approximately 3 at any temperature, with the highest value always obtained in *p*-dioxane. The variation in TOF did not correlate with either the solvent dielectric constant or its dipole moment. These catalysts deactivated by 1–2 orders of magnitude over a 24-h period at 298 or 373 K, presumably due to CO adsorption caused by a decarbonylation side reaction, and the total number of turnovers at 373 K was highest in ethanol and *p*-dioxane (ca. 2000), which gave conversions of 50–60%. At 423 K, the highest conversions after 24 h increased to about 95% (in ethanol or cyclohexanol). When compared at conversions near 30%, the solvent did not markedly influence the product distribution, although *p*-dioxane gave the lowest selectivity to geraniol and nerol. Lower citral concentrations lowered selectivity to these unsaturated alcohols, whereas H_2 pressure did not impart any significant trends. In these eight solvents, a one-half to first-order dependence on citral occurred, whereas the exponential dependence on H_2 pressure was relatively invariant around 0.3.

1. Introduction

In the pharmaceutical and specialty chemical industries, hydrogenation reactions play an important part in the manufacture of chemical intermediates. The application of heterogeneous catalysts has been increasing because of the virtues of easy separation from the organic media and catalyst reusability, which facilitate the use of continuous processes and the development of environmentally friendly processes. Reactions are carried out in a solvent for a various reasons, including to dissolve solid reactants and products, to control high reaction rates, to dissipate any reaction exothermicity, and to free the catalyst surface of site blockers; however, the solvent may have to be considered as a potential participant in the overall reaction kinetics. In organic syntheses, selective hydrogenation of α,β-unsaturated aldehydes forms a significant class of reactions, and traditionally $NaBH_4$ has been used as a stoichiometric reductant; however, supported metal catalysts have shown much promise for providing higher selectivity to unsaturated alcohols [1]. Most of the kinetic studies on hydrogenation of α,β-unsaturated aldehydes have been conducted in the vapor phase, whereas liquid-phase studies have focused mainly on rate and selectivity characteristics; thus issues due to the presence of the solvent in the reaction

* Corresponding author.
E-mail addresses: samrat.mukherjee@abbott.com (S. Mukherjee), mavche@engr.psu.edu (M.A. Vannice).
[1] Present address: Abbott Laboratories, N. Chicago, IL, USA.

0021-9517/$ – see front matter
doi:10.1016/j.jcat.2006.06.021

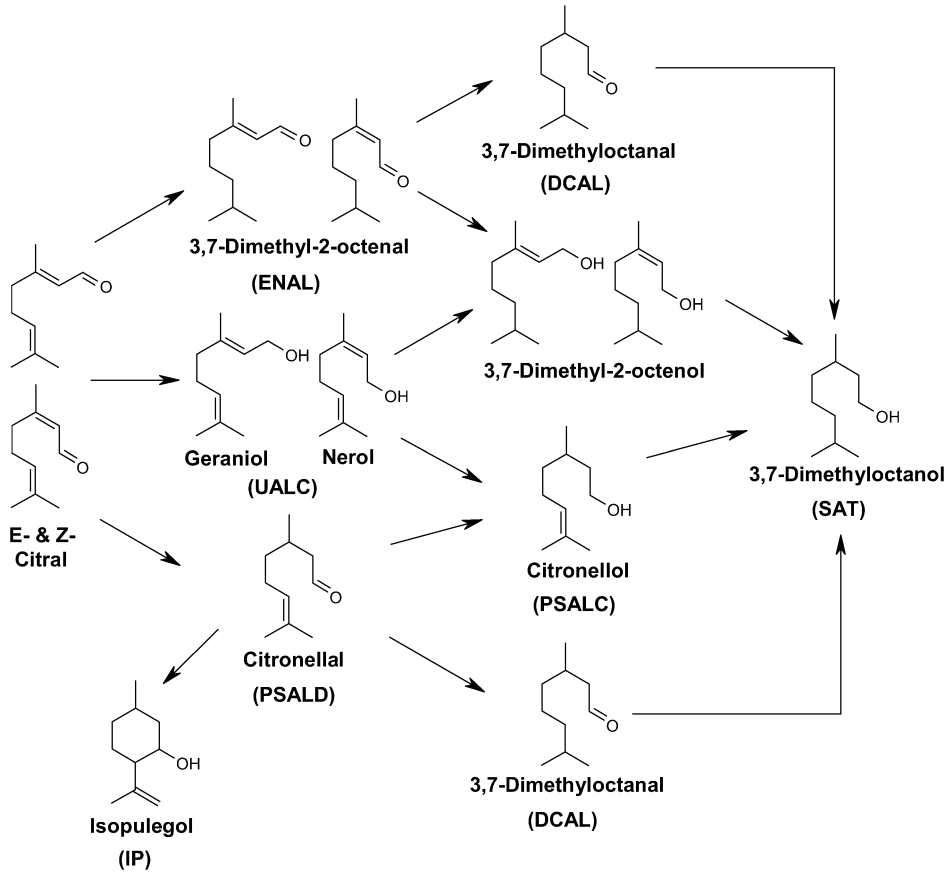

Fig. 1. Reaction chemistry network during citral hydrogenation.

system have seldom been addressed [2]. The liquid-phase hydrogenation of crotonaldehyde has been systematically studied by Lercher and co-workers [3,4], and citral hydrogenation in *n*-hexane has been thoroughly examined by Singh and Vannice [5–8]. The latter investigation showed that a catalyst reduced in situ can behave differently than one reduced ex situ [5].

Citral (3,7-dimethyl-2,6-octadienal) is a model α,β-unsaturated aldehyde with conjugated C=C–C=O bonds, as well as an additional isolated C=C double bond; thus a complex reaction network can exist, as shown in Fig. 1. Hydrogenation of the carbonyl group in the two (*E* and *Z*) stereoisomers of citral gives geraniol and nerol, respectively, whereas hydrogenation of the conjugated C=C bond yields citronellal, whose C=O bond can be hydrogenated further to citronellol. Reduction of all the double bonds yields the saturated compound 3,7-dimethyloctanol. Citronellal and citronellol are important perfumery chemicals, whereas geraniol and nerol are used as reactants in the synthesis of fine chemicals and special-property polymers [9]. The cyclization of citronellal produces isopulegol, which can be further hydrogenated to menthol—a commercially valuable compound. Production of the (-) menthol enantiomer is of particular interest; Iosif et al. recently reported a one-pot transformation of citronellal to menthol isomers with high selectivity using Ir/zeolite catalysts [10], whereas Trasarti et al. reported high yields of menthol from citral using metal/acid catalysts [11].

In the present investigation, the kinetic properties of liquid-phase citral hydrogenation on a Pt/SiO_2 catalyst were carefully examined in eight different solvents: *n*-amyl acetate, ethanol, ethyl acetate, cyclohexanol, cyclohexane, *n*-hexane, *p*-dioxane, and tetrahydrofuran (THF). These solvents were selected to provide a wide range of different properties, such as polarity, dielectric constant, and viscosity. Numerous tests using the Weisz–Prater (WP) criterion verified the absence of mass transfer limitations under our reaction conditions; procedural details to determine the molecular properties required for these evaluations are given in Appendix A. Catalytic behavior in the kinetic regime was then examined to determine the influences of these properties on specific activity and product selectivity.

2. Experimental

The SiO_2 (Davison Grade 57) used as a catalyst support had a BET surface area of 315 m^2/g, an average bulk density of 0.4 g/cm^3, and an average pore diameter of 14 nm. The silica granules were calcined under a constant flow of dry air at 773 K for 2 h in a quartz tube furnace. The Pt/SiO_2 catalyst was prepared via ion-exchange using $Pt(NH_3)_4(OH)_2{\cdot}xH_2O$ (Aldrich) as the Pt precursor. The SiO_2 was stirred for 4 h in a solution of the Pt precursor in double distilled water at a pH of 10 (using NH_4OH). The resulting catalyst was filtered and dried overnight in air in a furnace maintained at 393 K, then

ground and screened to a 60/100 mesh size and stored in a desiccator for later use [12]. A Pt loading of 3.15% was determined based on atomic adsorption spectrometry performed at the Materials Characterization Laboratory at Penn State University. The Pt/SiO_2 catalyst was reduced at 673 K under flowing H_2 for 75 min before a chemisorption experiment, evacuated, cooled to 300 K, and then characterized by either H_2 or CO chemisorption in a static volumetric apparatus providing a base pressure of 10^{-6} Torr. The measurements of both total and reversible uptakes were conducted at ambient temperature following standard procedures described elsewhere [13]. The H_2 (MG Ind., 99.999%) and CO (Matheson, 99.99%) were passed through molecular sieve traps (Supelco) and indicating Oxytraps (Alltech) for additional purification. X-ray diffraction (XRD) spectra were obtained for the fresh reduced catalyst using a Rigaku Geigerflex diffractometer equipped with a CuK_a radiation source and a graphite monochromator. The sample was first scanned for both the SiO_2 support and Pt peaks over a range of $2\theta = 90°$–$20°$ at a rate of $5° \text{ min}^{-1}$, and then a second scan was performed over a 2θ range of 42°–37° at a rate of $1° \text{ min}^{-1}$ for more accurate resolution of the most intense Pt peak at 39.77°.

The citral hydrogenation reactions were conducted in a system designed to include a 100-ml SS-autoclave (EZ-Seal, Autoclave Engineers), an automated H_2 pressure data acquisition system, a high-pressure syringe pump (ISCO 500D) to handle liquids, and various mass-flow sensors and pressure controllers [5]. About 0.1 g of the Pt/SiO_2 catalyst was placed in the reactor and purged with He (MG Industries, 99.999%) using five pressure-vent cycles of up to 54 atm to displace the air in the reactor and the lines. The reactor was also leak-tested at the peak He pressure to ensure a tight seal. The in situ pretreatment procedure consisted of heating the catalyst under a 200 cm^3 (STP)/min He flow to 673 K during a 3-h ramp, switching to a flow of 500 cm^3 (STP)/min H_2 for 75 min at the same temperature, cooling to room temperature, and then leaving the catalyst overnight under a H_2 pressure above 1 atm to ensure no air leakage into the reactor. Kinetic runs following this procedure provided the same results as runs conducted immediately after the pretreatment [5].

Care was taken to avoid traces of oxygen in the system. Citral and solvents were always degassed by bubbling N_2 (MG Industries, 99.999%) through them for 30 min before their use in the reaction. The reactor was pressurized with H_2 to the desired level, the solvent was fed via the air-tight syringe pump, and the reactor was raised to the desired reaction temperature. The high-purity solvents used in this study were *n*-amyl acetate (Acros, 99%), ethanol (Aldrich, 99.5%), ethyl acetate (Fisher, 99.9%), cyclohexanol (Aldrich, 99%), cyclohexane (Sigma–Aldrich, 99.9%), *n*-hexane (Fisher, 99.9% saturated C_6), 1,4-dioxane (Sigma–Aldrich, 99.9%), and tetrahydrofuran (THF) (Sigma–Aldrich, 99.9%). The catalyst/solvent slurry was allowed to equilibrate at reaction conditions with 1000-rpm agitation for 30–40 min before citral (Aldrich, 97.8% mixture of *cis*- and *trans*-isomers) was admitted into the reactor using the same syringe pump, to give a total liquid volume of 60 ml. Cyclohexanol is a very viscous liquid with a high melting point (293–295 K); thus, to avoid solvent deposition inside the syringe pump and the lines, a glass bubbler heated to 350 K was used to charge cyclohexanol to the reactor via gravity flow through a different set of transfer lines. During the addition of cyclohexanol, a low flow of H_2 through the reactor was maintained to prevent pressure buildup. The reaction conditions covered a range of temperature (298–423 K), pressure (10–30 atm) and citral concentration (0.5–5.9 M). The hydrogenation experiments were conducted in a semibatch mode with respect of H_2 by maintaining the reactor pressure within 5% of the set point using a Brooks 5860E pressure controller. Kinetic behavior in these different solvents was compared at standard reaction conditions 373 K, 20.0 atm H_2 pressure, and a citral concentration of 1.0 M unless stated otherwise.

Reactions were typically conducted for a 24-h period, during which time liquid samples (0.2–0.5 ml) were periodically withdrawn from the pressurized reactor through a dip tube, collected in a N_2-purged closed glass vessel, and subsequently analyzed using a HP 5890 gas chromatograph equipped with a thermal conductivity detector and a 10% Carbowax 20M-on-Supelcoport packed column. The initial oven temperature was set at 383 K, and a ramp of 1 K/min was applied for a run time of 33 min, with injector and detector temperatures at 473 and 513 K, respectively. The solvents eluted at the beginning of the chromatogram and did not interfere with the peaks for citral and its derivatives. The GC data were processed using a HP 3396 integrator, and the compositions were determined using molar response factors that were obtained for different components under similar conditions [5]. To verify the absence of any products formed by a reaction of the solvent itself, liquid samples from these experiments were analyzed by GC-MS at the Department of Chemistry, Penn State University.

3. Results

The H_2 and CO chemisorption experiments with the 3.15% Pt/SiO_2 catalyst gave irreversible uptakes at 300 K, corresponding to ratios of $H/Pt_t = 1.27$ and $CO/Pt_t = 0.77$, where Pt_t is the total moles of Pt [12]. Consequently, a dispersion (Pt_s/Pt_t) of unity was assumed for the catalyst, indicating 1.1-nm Pt crystallites [14]. The small Pt crystallite size was confirmed by the absence of any major Pt peaks in the X-ray diffraction spectrum of the catalyst [12].

The solvents used in this study had a wide range of volatility; therefore, the total reactor pressure during the hydrogenation runs was corrected for the vapor pressure of the citral–solvent mixture at the reaction temperature to determine the actual H_2 partial pressure. Each solvent vapor pressure was computed using the Antoine equation [15], whereas the vapor pressure of citral at temperatures from 335 to 501 K was obtained from Perry's Chemical Engineers' Handbook [16]. These corrections were not significant at 298 K (<0.5%) for even the most volatile solvent on the list; however, at higher temperatures, significant errors in the reaction order could occur if these corrections—sometimes as high as 45%—were not made [12].

Before the citral hydrogenation experiments, blank runs were performed with each solvent using either no catalyst or

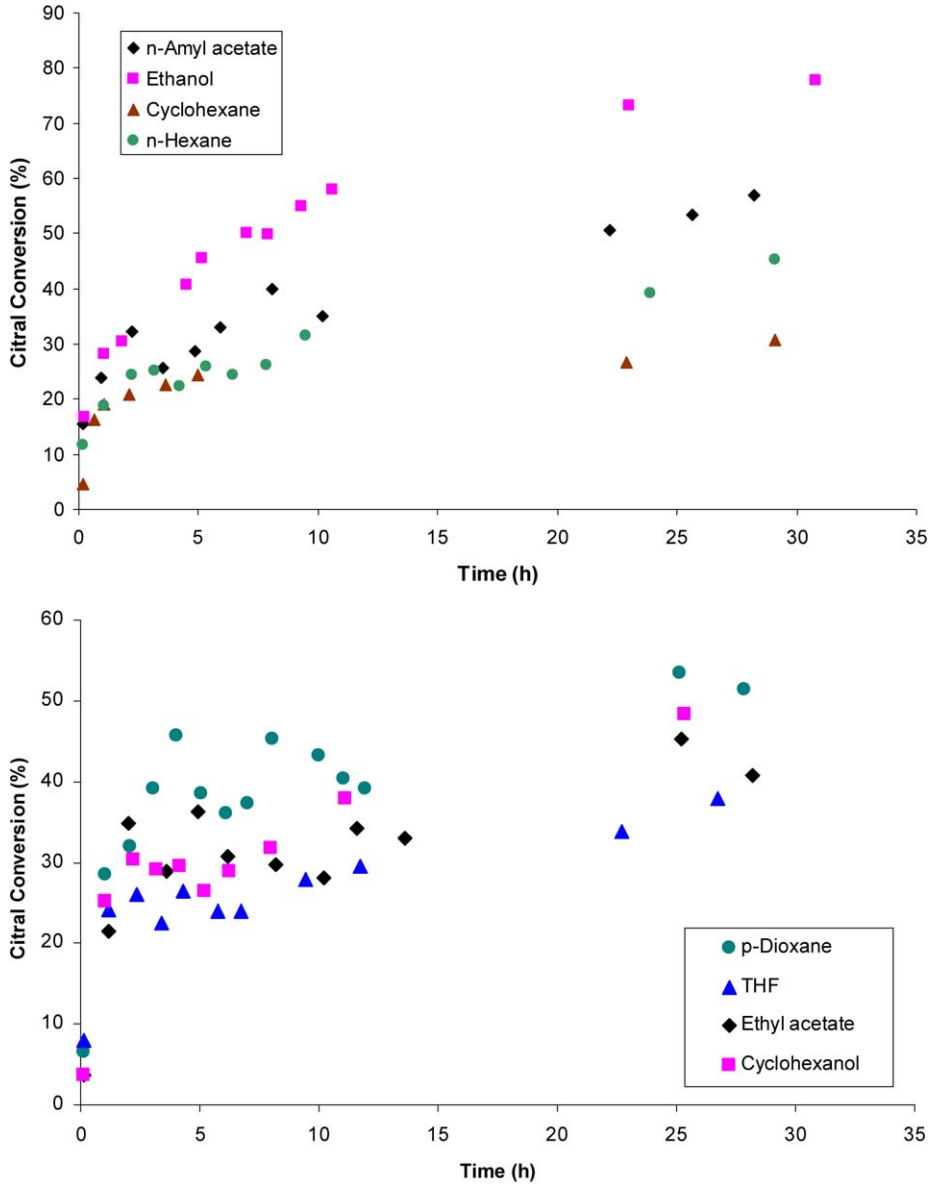

Fig. 2. Citral conversion vs time in different solvents. Initial reaction conditions: 373 K, 20 atm H_2, 1 M citral.

no citral. In the absence of a catalyst, no change in the initial concentration of citral was observed after long periods, up to 5 h. With no citral in the reactor, the catalyst showed no activity, as indicated by the H_2 consumption. Furthermore, GC-MS analyses showed no evidence of any reaction between citral and the solvent.

Fig. 2 shows representative conversion time profiles for citral hydrogenation in the eight solvents at 373 K, 20 atm H_2 pressure, and 1 M citral concentration. The characteristics at different stages of the reaction were dependent on the solvent used in the reaction; however, initial rates were determined from the time derivative of the citral concentration for conversions $<20\%$. Usually, each run was repeated at least once, and an average activity was calculated. Table 1 lists the initial turnover frequency (TOF-molecule s^{-1} Pt_s^{-1}) obtained in the eight solvents at 298, 373, and 423 K at standard conditions of 1 M citral and 20 atm H_2 pressure, as determined from plots illustrated in Fig. 2 [12]. A 2.5-fold variation in the initial TOF occurred among the solvents at 373 K, whereas at 298 and 423 K, the TOF varied by a factor of 3 and 3.4, respectively, with the highest and lowest values obtained with *p*-dioxane and *n*-amyl acetate, respectively. Initial rates at 298 K were routinely found to be higher than those at 373 and 423 K, and this unusual temperature effect was observed with every solvent, but normal Arrhenius behavior existed above 373 K. Such behavior has been reported previously for citral hydrogenation on a Pt/SiO_2 catalyst with *n*-hexane as the solvent, and it has been attributed to a decomposition side reaction that produces an inhibitor, that is, CO [5]. The activity characteristics of citral hydrogenation in each solvent at 373 K were analyzed over an extended reaction period, and the results after 24 h are also presented in Table 1. Each TOF describing the instantaneous reaction rate at $t = 24$ h is 1–2 orders of magnitude lower than the corresponding initial value. The highest citral conversion,

Table 1
Average initial TOF values (±0.02) for citral hydrogenation on 3.15% Pt/SiO_2 in different solvents

Solvent	Initial TOF (s^{-1})[a]			After 24 h at 373 K		
	298 K	373 K	423 K	X_{cit}	Total # of turnovers[b]	TOF (s^{-1})[c]
n-Amyl acetate	0.22	0.11	0.16	40	1420	0.0062
Ethanol	0.45	0.13	0.21	62	2190	0.0098
Ethyl acetate	0.46	0.18	0.34	42	1540	0.0057
Cyclohexanol	–	0.25	0.34	48	1700	0.0087
Cyclohexane	0.38	0.13	0.27	32	1150	0.0010
n-Hexane	0.39	0.15	0.20	30	1080	0.0021
p-Dioxane	0.62	0.26	0.55	52	1880	0.0084
THF	0.34	0.19	0.25	34	1210	0.0026

[a] 20.0 atm H_2, 1 M citral.
[b] Based on the average TOF over 24 h of reaction.
[c] Based on the instantaneous reaction rate at $t = 24$ h.

representing a total turnover of 2190 molecules per site after 24 h, was obtained with ethanol, whereas only half as much citral had reacted under the same conditions with cyclohexane or *n*-hexane as the solvent, as indicated in Fig. 2. This occurred even though the initial rates were the same as or higher than that with ethanol as the solvent.

The product distribution was monitored as the conversion increased with time, and representative behavior is illustrated in Figs. 3a–3c for ethanol at the three different temperatures. Similar plots for all runs are provided elsewhere [12]. The product selectivities (S_i) were determined from the instantaneous molar concentration (C_i) of each product at a given time and are expressed as

$$S_i = C_i / \sum_{i=\text{products}} C_i = C_i / C_{0,\text{cit}} X_{\text{cit}}, \quad (1)$$

where $C_{0,\text{cit}}$ and X_{cit} are the initial citral concentration and the instantaneous citral conversion, respectively. Geraniol and nerol have been combined as unsaturated alcohols (UALC), ENAL represents the two isomers of 3,7-dimethyl-2-octenal, whereas PSALD and PSALC represent the partially saturated aldehyde (citronellal) and the partially saturated alcohol (citronellol), respectively. IP and DCAL stand for isopulegol and dihydrocitronellal, respectively, while the completely saturated compound, 3,7-dimethyloctanol, is designated as SAT. Product distributions from plots such as those in Figs. 3a–3c at similar conversions of approximately 30% are listed in Tables 2–4 for 298, 373, and 423 K, respectively. Hydrogenation of only the C=O bond was heavily favored at the two higher temperatures, with the selectivity to unsaturated alcohols (UALC) frequently exceeding 70% at these "lower" conversions. This selectivity increased with conversion and ranged from 68% to 84% at 373 K and from 70% to 83% at 423 K, with the exception of cyclohexanol [12]. In contrast, at 298 K hydrogenation of the C=C bonds became more pronounced and secondary hydrogenation reactions became more prevalent with time even though initial selectivities to UALC, PSALD, and PSALC were comparable at 298 and 373 K. This trend is visible in Figs. 3a–3c. At either 298 or 373 K, the formation of SAT appeared to be restricted to the early stages of reaction because selectivity to SAT decreased at higher citral conversions.

Citral hydrogenation reactions were also conducted at varying citral concentrations (0.5–3.0 M) and H_2 pressures (10–30 atm) in each solvent at 373 K to examine the differences in the product distribution and to study the dependence of the initial TOF on reactant concentrations [12]. The selectivity results at low and high citral concentrations and 20 atm H_2 are listed in Table 5, and similar results at an initial citral concentration of 1 M and lower and higher H_2 pressures are given in Table 6. The power law reaction orders obtained are listed in Table 7. These ln–ln plots are shown later along with the fits of the reaction model [17]. In addition, similar runs were also conducted at 298 and 423 K with cyclohexane or ethyl acetate as the solvent so that the thermodynamic behavior of the adsorption equilibrium constants could be examined. Representative results are shown in Figs. 4 and 5 for the latter two solvents. All data used for kinetic modeling were verified to be free of mass transfer limitations (see Appendix A).

4. Discussion

In a heterogeneously catalyzed system, the concept of a turnover frequency at a specified set of reaction conditions is very useful because it normalizes rate data for comparative studies. This 3.15% Pt/SiO_2 catalyst gave H/Pt_t ratios well above 1 and had CO/Pt_t ratios close to 0.8, both of which indicate a high Pt dispersion near unity [14]; thus a dispersion value of 1.0 was used to calculate TOFs. To compare solvent effects during citral hydrogenation conducted in this semibatch reactor, the initial TOF was picked to represent maximum activity, not only because the reaction conditions are the most well defined, but also because any inhibition due to side reactions is minimized. With a porous catalyst, intraparticle diffusion limitations can play a significant role in determining the overall kinetics of the reaction, and it is imperative that rate data used for reaction modeling be obtained in the regime of kinetic control. Determining criteria such as a Weisz–Prater number or a Thiele modulus to evaluate mass transfer effects, especially pore diffusion, can be complicated for complex reactant (or solvent) molecules, because their experimentally measured bulk diffusivities, D_b, have rarely been reported. In a liquid-phase system, these parameters are needed to estimate effective diffusivities, D_{eff}, within the pore structure of the catalyst. However,

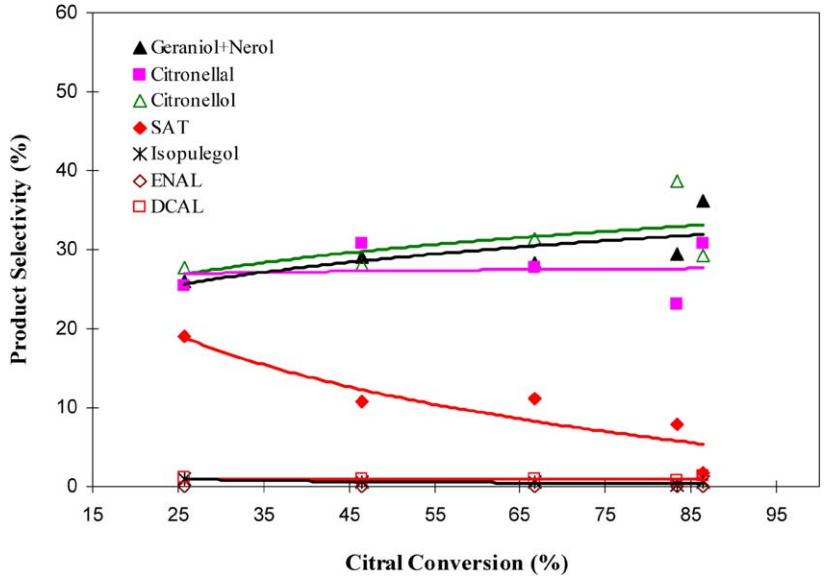

(a)

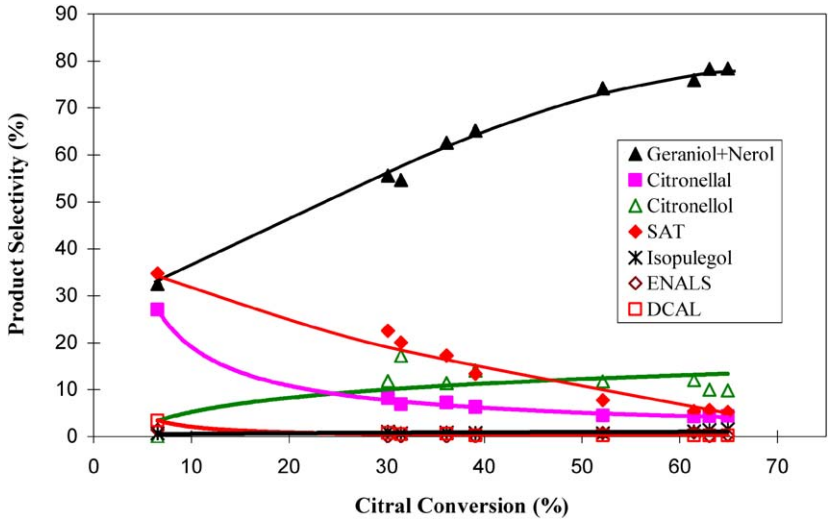

(b)

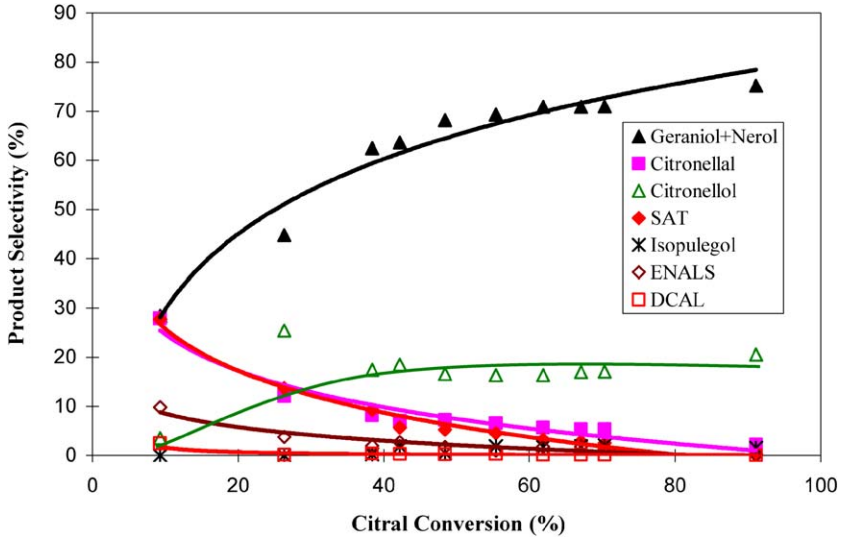

(c)

Fig. 3. Product selectivity during citral hydrogenation in ethanol at 20 atm H_2 and an initial concentration of 1 M citral: (a) 298 K, (b) 373 K, (c) 423 K.

Table 2
Product selectivity (mol%) during citral hydrogenation in different solvents

Solvent	X_{cit}[a]	UALC	PSALD	IP	ENAL	PSALC	DCAL	SAT
n-Amyl acetate	32	16	23	0	7	38	2	14
Ethanol	26	26	25	1	0	28	1	19
Ethyl acetate	33	12	19	4	6	40	1	18
Cyclohexanol								
Cyclohexane	30	16	16	4	7	21	3	33
n-Hexane	32	16	19	3	7	39	2	14
p-Dioxane	37	25	28	5	8	23	2	10
THF	37	15	41	3	4	25	2	10

Note. Reaction conditions: 298 K, 20 atm H_2, and 1 M citral. (See Fig. 1 for abbreviations.)
[a] Citral conversion.

Table 3
Product selectivity (mol%) during citral hydrogenation in different solvents

Solvent	X_{cit}	UALC	PSALD	IP	ENAL	PSALC	DCAL	SAT
n-Amyl acetate	33	49	31	1	0	16	0	3
Ethanol	30	56	8	1	0	12	1	22
Ethyl acetate	33	72	9	1	1	14	0	3
Cyclohexanol	32	73	11	1	0	13	0	2
Cyclohexane	31	74	7	1	0	12	1	5
n-Hexane	31	73	10	1	3	8	1	4
p-Dioxane	32	27	10	1	0	42	0	20
THF	30	78	5	1	1	11	0	4

Note. Reaction conditions: 373 K, 20 atm H_2, and 1 M citral. (See Fig. 1 for abbreviations.)

Table 4
Product selectivity (mol%) during citral hydrogenation in different solvents

Solvent	X_{cit}	UALC	PSALD	IP	ENAL	PSALC	DCAL	SAT
n-Amyl acetate	31	69	7	2	2	16	0	4
Ethanol	38	62	8	0	2	18	1	9
Ethyl acetate	28	78	7	2	2	8	0	3
Cyclohexanol	30	68	15	2	1	12	0	2
Cyclohexane	31	71	8	1	2	10	0	8
n-Hexane	32	81	6	1	0	9	1	2
p-Dioxane	30	60	7	1	0	29	0	3
THF	33	83	7	1	0	7	0	2

Note. Reaction conditions: 423 K, 20 atm H_2, and 1 M citral. (See Fig. 1 for abbreviations.)

Table 5
Product selectivity (mol%) in different solvents at different initial citral concentrations

Solvent	X_{cit}	UALC	PSALD	IP	ENAL	PSALC	DCAL	SAT
				(a) At 0.5 M citral				
n-Amyl acetate	30	22	18	0	0	16	0	44
Ethanol	34	22	10	1	2	35	1	29
Ethyl acetate	34	34	10	1	0	43	0	12
Cyclohexanol	32	28	15	1	0	40	0	16
Cyclohexane	31	35	15	1	3	24	0	22
n-Hexane	32	30	7	1	0	26	1	35
p-Dioxane	36	7	16	0	0	21	0	56
THF	33	34	9	1	0	43	1	12
				(b) At 3.0 M citral				
n-Amyl acetate	13	76	7	1	0	11	0	5
Ethanol	23	79	8	1	0	6	0	6
Ethyl acetate	26	65	7	2	1	22	0	3
Cyclohexanol	24	87	5	1	0	5	0	2
Cyclohexane	17	53	4	3	0	37	1	2
n-Hexane	23	70	3	1	0	20	0	6
p-Dioxane	31	42	5	2	0	47	0	4
THF	20	68	8	3	1	12	0	8

Note. Reaction conditions: 373 K and 20 atm H_2. (See Fig. 1 for abbreviations.)

Table 6
Product selectivity (mol%) in different solvents at different H_2 pressures

Solvent	X_{cit}	UALC	PSALD	IP	ENAL	PSALC	DCAL	SAT
				(a) 10 atm H_2 pressure citral				
n-Amyl acetate	12	52	10	2	0	25	0	11
Ethanol	28	54	13	2	3	15	2	11
Ethyl acetate	27	32	8	2	0	48	0	10
Cyclohexanol	32	37	6	1	0	50	0	6
Cyclohexane	19	61	10	3	0	20	1	5
n-Hexane	23	49	5	1	1	37	0	7
p-Dioxane	22	28	12	1	0	38	0	20
THF	24	29	5	1	0	53	0	12
				(b) 30 atm H_2 pressure				
n-Amyl acetate	27	57	15	1	2	22	0	3
Ethanol	37	56	11	0	0	16	1	16
Ethyl acetate	35	60	8	1	1	27	0	3
Cyclohexanol	32	47	12	1	0	33	0	7
Cyclohexane	24	66	9	2	0	18	1	4
n-Hexane	33	54	5	1	1	28	2	9
p-Dioxane	29	10	12	1	0	33	0	44
THF	36	38	5	0	0	45	0	12

Note. Reaction conditions: 373 K and 1 M citral initially. (See Fig. 1 for abbreviations.)

methods exist that allow determination of the physical properties required to calculate D_b values, including critical temperature and pressure, density, viscosity, vaporization enthalpy, as well as calculating a Henry's law constant. The use of these approaches to estimate bulk diffusivities and gas solubilities is discussed in Appendix A. Once bulk diffusivity is known, an effective diffusivity can be estimated that, when combined with a measured reaction rate, a known reactant concentration, and a determined value of the catalyst particle radius, allows calculation of a Weisz–Prater (WP) number, as also shown in Appendix A. This value indicates whether or not pore diffusion limitations are significant [14]. In this study, numerous tests using the WP criterion verified that all data for each solvent were obtained in the regime of kinetic control; for example, WP values at 373 K ranged from $\varnothing_{WP} = 0.0032$ to 0.013 for H_2 and $\varnothing_{WP} = 0.0034$ to 0.035 for citral, as shown in Table A.8 in Appendix A. Earlier tests using the Madon–Boudart method [18] with *n*-hexane as the solvent also confirmed this finding [5].

Pd has been reported to be the most active group VIII metal for citral hydrogenation [8]. This reaction was examined in four solvents by Aramendia et al. using a 3% Pd/SiO_2–$AlPO_4$ catalyst [19]. At the conditions listed in Table 8, the much lower rate of citral hydrogenation on Pd in methanol was attributed by Aramendia et al. to be a steric effect caused by the formation of citronellal acetals and diacetals via a reaction between methanol and citral. Neri et al. also reported the formation of citronellal acetals in significant quantities during citral hydrogenation in ethanol using different supported Ru catalysts; however, significant acetal formation (up to 70% yields) was observed only with catalysts prepared from a Cl-containing Ru precursor, whereas yields were <1% when $Ru(NO)(NO_3)_3$ was the precursor [20]. Acetal formation from an alcohol and an aldehyde is acid-catalyzed, and Neri et al. demonstrated that acidic sites on the support, created by the presence of Cl^- [21,22], led to the formation of these acetals [20]. Thus, use of a chloride precursor can be a major factor in acetal byproduct formation and, because Aramendia et al. used Na_2PdCl_4, their explanation of the lower rate with CH_3OH as a solvent is probably correct. In our study, the Pt/SiO_2 catalyst contained no Cl, and no spectroscopic evidence of acetals was found in the reaction mixture at the end of the reaction using ethanol as the solvent. The periodic gas chromatograms obtained during the reaction also showed no components other than those obtained with nonalcoholic solvents. Thus, although solvent–substrate reactions during citral hydrogenation may manifest themselves with specific solvents under certain reaction conditions, no evidence for such reactions was observed in the kinetic runs reported here.

Table 7
Power law rate dependency on citral concentration and hydrogen pressure $r = C_{cit}^{x} P_{H_2}^{y}$

Solvent	T (K)	x	y
n-Hexane	373	0.56	0.41
n-Amyl acetate	373	0.83	0.31
p-Dioxane	373	0.50	0.27
Cyclohexanol	373	0.46	0.42
THF	373	0.80	0.36
Cyclohexane	373	0.80	0.29
Ethyl acetate	373	0.50	0.23
Ethanol	373	0.56	0.39
Cyclohexane	298	0.64	0.22
Cyclohexane	423	0.69	0.37
Ethyl acetate	298	0.43	0.17
Ethyl acetate	423	0.73	0.23

In organic chemistry, the electronic properties of the solvent can alter the mechanistic aspects of a reaction, and this capability has been associated with a change in the free energy state of the reactants, which can alter the favorability of different reaction paths in these homogeneous systems. With heterogeneous catalysts, the solvation of reacting species and its impact on the overall kinetic mechanism are not clearly understood. However, in a study of polar and nonpolar reactants, it has been stated

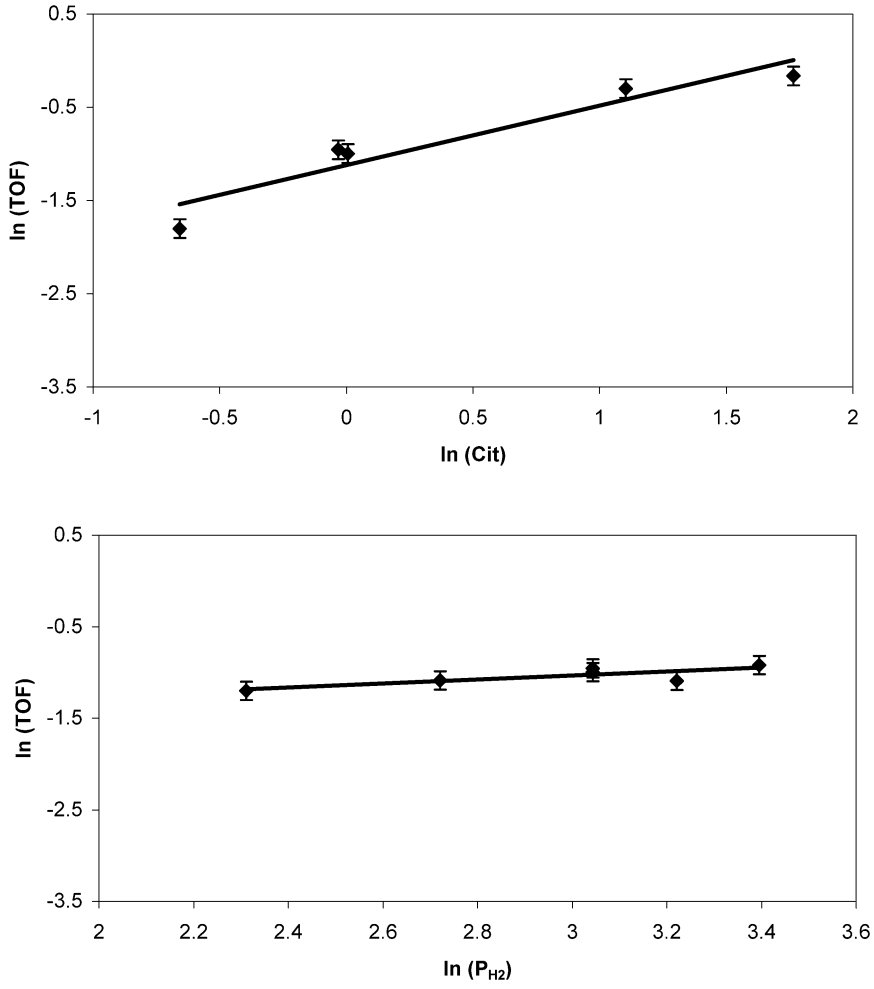

(a)

Fig. 4. Dependence of initial TOF for citral concentration (at 20 atm H_2) and H_2 pressure (at 1 M citral) for citral hydrogenation on 3.15% Pt/SiO_2 in cyclohexane: (a) 298 K, (b) 373 K, (c) 423 K.

Table 8
TOF for citral hydrogenation on a 3% Pd/SiO_2–$AlPO_4$ catalyst in different solvents [19]

Solvent	Dielectric constant, ε	TOF (s^{-1})			
		293 K	303 K	313 K	323 K
Cyclohexane	2.0	4.5	6.9	8.1	10
p-Dioxane	2.2	7.9	8.6	9.6	10
THF	7.6	2.3	3.0	3.3	5.8
Methanol	33	0.59	0.76	1.5	2.1

Note. Reaction conditions: 4 atm H_2, 0.5 M citral, Pd dispersion = 18%.

that hydrogenation of less polar substrates in more polar solvents (and vice versa) is preferred [23]. The solvents used in our study exhibit a 13-fold variation in dielectric constants, whereas their dipole moments vary from 0 to 1.9 Debye [15,24]. The initial TOF for citral hydrogenation in different solvents did not show a correlation at any temperature with either the solvent dielectric constant or its dipole moment; the results at 373 K are presented in Fig. 6 as an example. The data are presented in an order of increasing solvent dielectric constant; the two solvents that most noticeably fail to correlate the initial TOF with the dielectric constant are *p*-dioxane and ethanol. Aramendia et al. also found that the highest rate of citral hydrogenation on a Pd/SiO_2–$AlPO_4$ catalyst was obtained with *p*-dioxane as the solvent and no smooth trend of activity versus dielectric constant was observed, consistent with our results given in Table 6 [19].

The electronic properties of a compound traditionally have been represented by either the dielectric constant or the permanent dipole moment. Although these quantities are not directly related to each other, they have been routinely used in the literature to characterize solvents as either polar or nonpolar [25]. The dielectric constant (or the relative permittivity) is a macroscopic material property that plays an important role in the characterization of solvents due to the simplicity of solvation models based on an electrostatic continuum. Unfortunately, these models fail to distinguish between truly nonpolar solvents (e.g., cyclohexane), which have a molecular structure devoid of any polar chemical bonds, and nondipolar solvents (e.g., benzene), which exhibit neutral behavior in electrostatic measurements despite the presence of polar bonds within the molecule. 1,4-Dioxane is yet another example of a nondipolar molecule that has a net zero dipole moment, due to symmetry, but still has polar chemical bonds, which can result

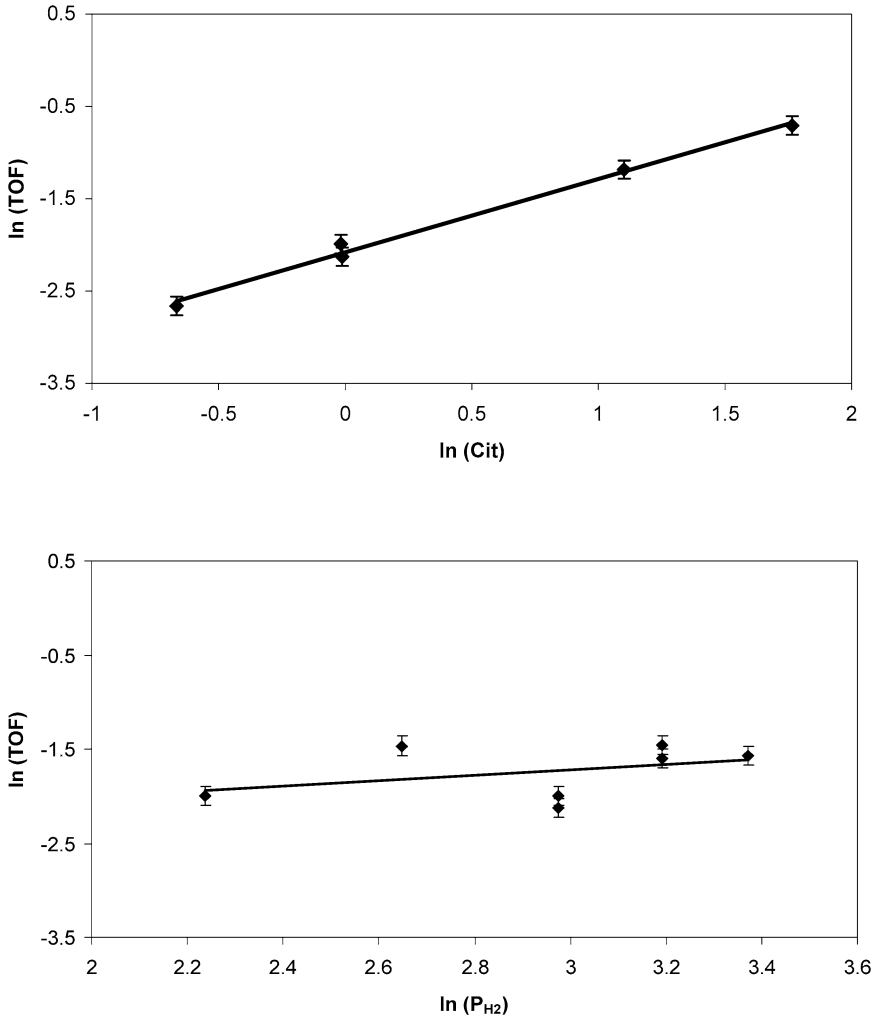

(b)

Fig. 4. (*continued*)

in higher-order multipole moments. The interaction of solutes with higher-order multipole moments (quadrupole, octupole, etc.) can be significant in certain cases, and this may apply in the case of a nondipolar solvent interacting with an adsorbed species on the catalyst surface. These higher-order multipole moments can have a significant effect on the thermodynamic properties of simple polyatomic fluids, as shown by Gubbins and Twu [26,27], and the presence of a quadrupole moment can increase the magnetic relaxation rate of the nucleus, as shown by an NMR study of Xe^{131} in dioxane [28–30]. Thus it is possible that these higher-order moments could affect kinetic behavior.

TOFs for citral hydrogenation at 373 K after 24 h of reaction in different solvents were more than an order of magnitude smaller than the corresponding initial TOF values, as shown in Table 1. However, at these conditions of lower rate and lower citral concentration, the WP numbers were even smaller, and no transport limitations existed [12]. Evidence exists that side reactions involving the decarbonylation of unsaturated alcohols and/or aldehydes can produce CO in situ, which can act as an inhibitor, especially at the lowest temperature of 298 K [3–5]. This behavior was first observed with *n*-hexane as the solvent [5], and it is very likely that similar behavior in the other solvents is the principal reason for the decreased rates resulting in conversions far below 100% after 24 h. Fig. 2 shows that the temporal activity characteristics at 373 K can vary significantly, depending on the solvent. As just mentioned, some of the activity decrease can be associated with catalyst deactivation; therefore, one solvent effect could be that influencing the extent of side reactions and/or the chemisorption of side reaction byproducts on the metal. The purest solvents available were used in these hydrogenation experiments, and no evidence of solvent impurities resulting in catalyst deactivation was observed. The initial TOF in either ethanol or cyclohexane was the same (0.13 s^{-1}), but as the reaction progressed, substantially more deactivation occurred with cyclohexane. Table 1 indicates that the total number of turnovers after 24 h in the different solvents decreased in the following order: alcohols > dioxane > acetates > THF > alkanes. Lercher et al. reported a complete loss of catalytic activity with Pt/SiO_2 catalysts after witnessing a high initial activity for crotonaldehyde hydrogenation, and also found that ethanol gave the highest final conversions [3]. Thus alcohols appear to maintain a cleaner catalyst surface during the liquid-phase hydrogenation of α,β-

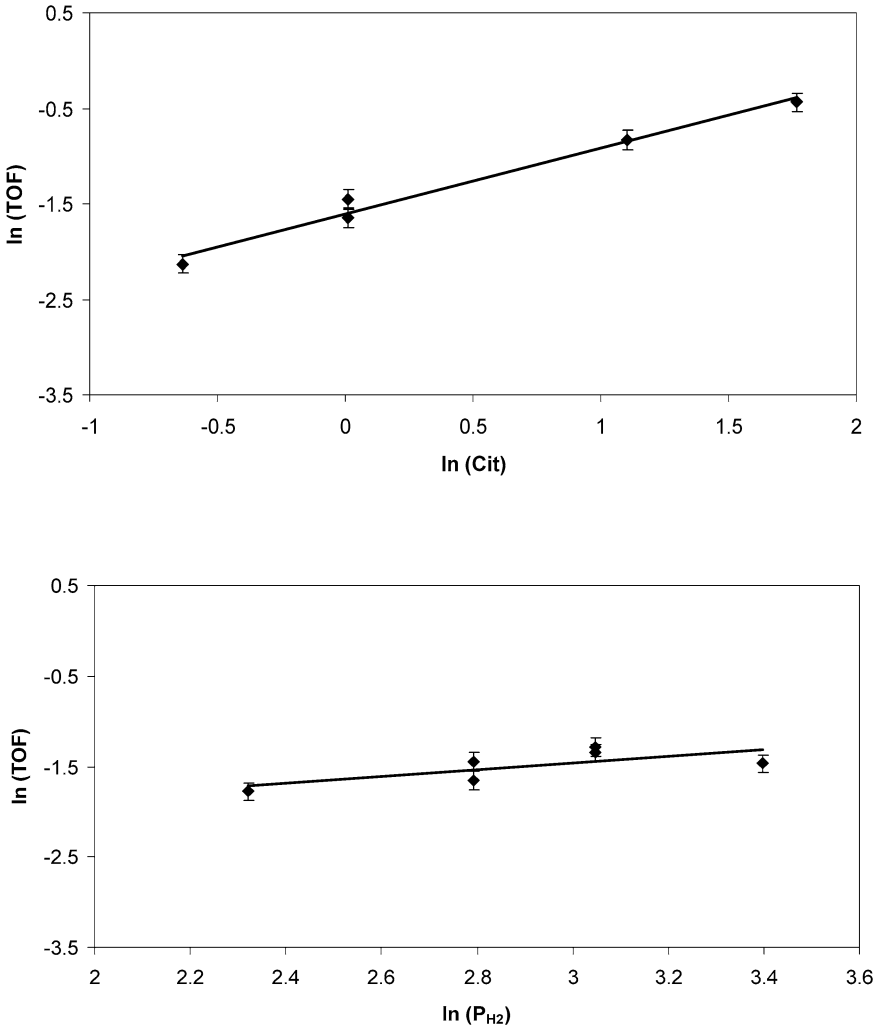

(c)

Fig. 4. (*continued*)

unsaturated aldehydes on Pt/SiO_2 catalysts and to yield higher conversions.

Arrhenius plots using the initial activities did not exhibit normal behavior; with each solvent, the activity at 298 K was always the highest, although the activity at 423 K was always higher than that at 373 K, as expected. This trend has been reported and discussed earlier and has been attributed to CO coverage of the Pt surface; at 373 K and above, CO produced from a side reaction can desorb and equilibrate to provide free metal sites [5]. Based on the initial TOFs at 298 and 373 K presented in Table 1 and the TOF at each temperature after 24 h, the relative deactivation in each solvent can be compared, as shown in Fig. 7. The total height of each bar represents the initial TOF, and the filled bars represent the instantaneous TOF after 24 h of reaction. Clearly, the relative decrease in TOF is far greater than expected due to the decrease in citral concentration, and catalyst deactivation is more pronounced at 298 K than at 373 K. This is consistent with the irreversibility of CO adsorption at 298 K, with the result that Pt sites are continuously, but more slowly, blocked by CO at 298 K, whereas the onset of reversible adsorption at the higher temperature results in a lower concentration of adsorbed CO but it is achieved more rapidly [5]. The highest conversions after 24 h were attained at 423 K, with values of 96, 94, and 82% obtained with cyclohexanol, ethanol, and *p*-dioxane, respectively. The first two are among the most polar solvents and have the highest dielectric constants.

Results such as those shown in Figs. 3a–3c illustrate how the cumulative product distribution changes with conversion, that is, with reaction time over a 24-h period. Although the reaction network is complicated, some general observations can be made, based on the selectivity values in Tables 2–4, regarding performance after a conversion of approximately 30%. First, at the two higher temperatures, initial hydrogenation of the carbonyl bond to form geraniol and nerol is clearly preferred to hydrogenation of the conjugated C=C bond to give citronellal, and almost no hydrogenation of the isolated C=C bond occurs to give dimethyloctenal. At higher conversions, selectivity to the unsaturated alcohols rises; for example, it ranges from 70 to 80% among all solvents at 373 K [12]. Second, selectivities are not widely divergent at 423 K, although *p*-dioxane and ethanol produce the lowest amount of the unsaturated alco-

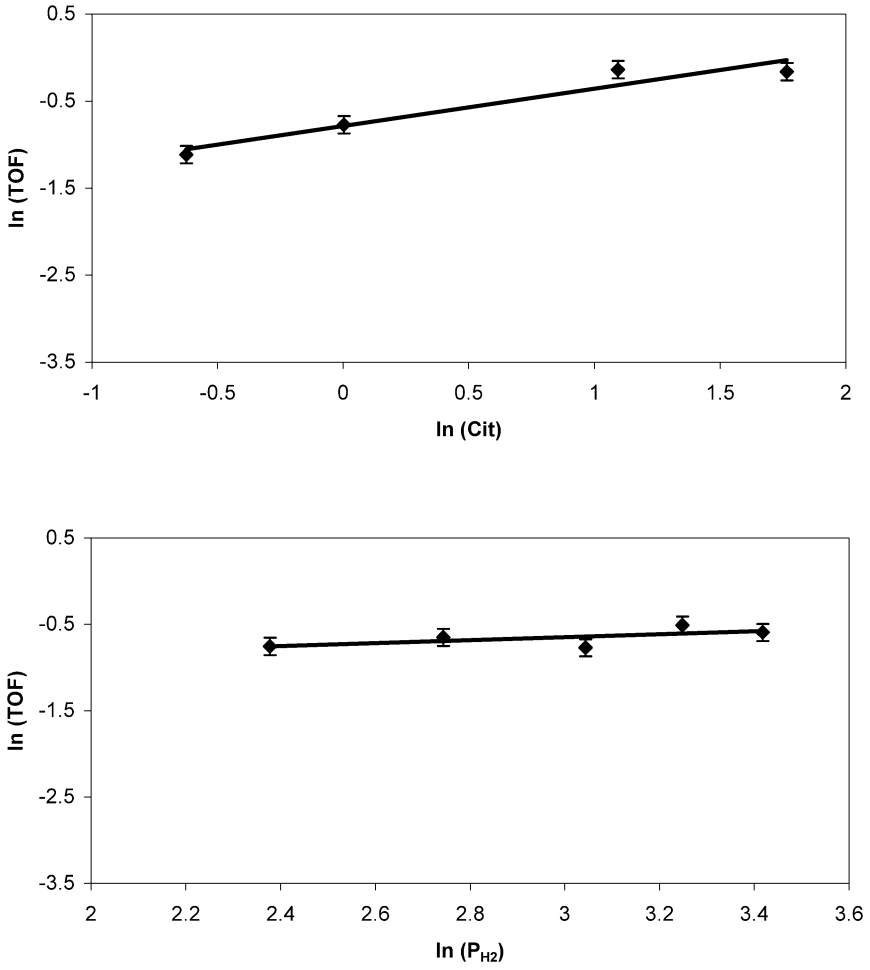

(a)

Fig. 5. Dependence of initial TOF on citral concentration (at 20 atm H_2) and H_2 pressure (at 1 M citral) for citral hydrogenation on 3.15% Pt/SiO_2 in ethyl acetate: (a) 298 K, (b) 373 K, (c) 423 K.

hol and favor its subsequent hydrogenation to citronellal. This pattern is even more pronounced at 373 K with *p*-dioxane, and, moreover, selectivity to geraniol and nerol is also lower with ethanol or *n*-amyl acetate as the solvent. Third, a significant capability to completely hydrogenate citral to the saturated product appears to be restricted to the use of ethanol or *p*-dioxane as solvent; however, it is not clear why these two solvents favor the readsorption and hydrogenation of the intermediate products. Fourth, conducting the reaction at 298 K shifted the selectivity from the unsaturated alcohols toward citronellal, favored subsequent hydrogenation to give citronellol and the saturated product dimethyloctanol, and enhanced hydrogenation of the isolated C=C bond. At 298 K, larger amounts of isopulegol were also detected in all solvents except *n*-amyl acetate. An earlier study demonstrated that a side reaction to deactivate this Pt catalyst via CO formation is attributable to geraniol and/or nerol, rather than to citronellal [6]. If so, then this shift in selectivity would enhance activity maintenance, which could explain the higher initial rates at 298 K, and the cleaner Pt surface could facilitate the sequential hydrogenation of the intermediate products, especially citronellal and citronellol.

A comparison of the product distributions represented in Tables 3, 5, and 6 indicates that the selectivity to UALC (geraniol and nerol) is lowest at low citral concentrations and increases with the citral concentration, especially with *n*-amyl acetate, ethanol, cyclohexanol, and *p*-dioxane. Further hydrogenation of the initial intermediates is clearly favored at low citral concentrations, especially to form the saturated product. This is most likely because competitive adsorption of the intermediates versus citral is enhanced. The selectivity to PSALD (citronellal) seems to be minimized at higher citral concentrations. Clear general trends are not obvious at 1 M citral as H_2 pressure increases. At 20 atm H_2, selectivity to UALC seems to be maximized, except for *n*-amyl acetate and *p*-dioxane, and the amount of PSALC (citronellol) is minimized, except with *p*-dioxane.

These results show, in agreement with previous studies [7,8,31–35], that the network of reactions describing the hydrogenation of citral and its intermediates provides a very informative model system to probe the influence of a specific metal or a particular support on the selectivity to a given product. However, much additional information related to the rate and adsorption constants for the sequential reactions is needed to accurately

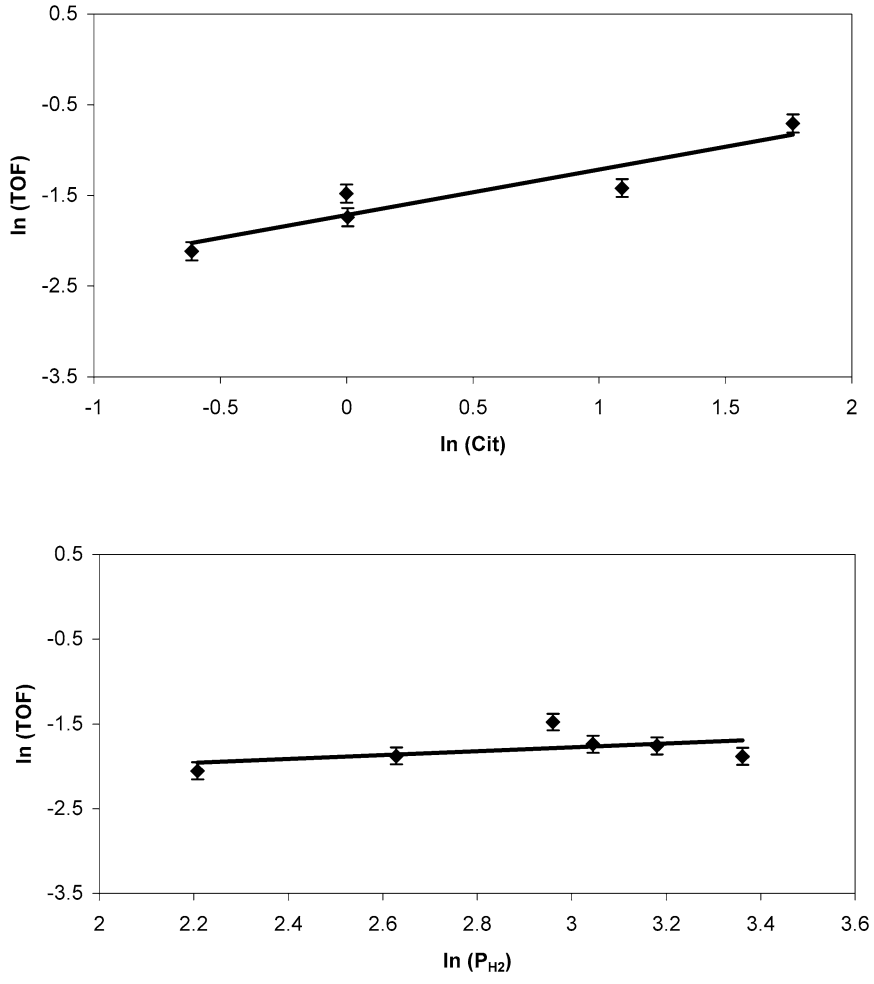

(b)

Fig. 5. (*continued*)

model this family of reactions. In the absence of these parameters, the simplest expression for citral hydrogenation in these solvents is a power law rate, $r = kC_{\text{cit}}^{x}P_{\text{H}_2}^{y}$, and plots such as those shown in Figs. 4 and 5 provide the x and y values listed in Table 7. As the initial citral concentration was increased from 0.5 to 5.9 M, the TOF also showed an increase in all of the solvents. The power law rate dependence on citral concentration was not zero-order, as was observed in many (if not most) liquid-phase hydrogenation reactions, but ranged from 0.45 to 0.85 depending on the solvent. The highest concentration of 5.9 M represents neat citral, and the initial TOF at 20 atm H_2 corresponding to that condition (0.49 s^{-1} at 373 K) was greater than that obtained with any solvent. These results indicate a Pt surface not completely saturated with adsorbed citral. Over a hydrogen pressure range of 10–30 atm, the initial TOF showed a lower exponential dependence on P_{H_2} of 0.2–0.4 with the eight solvents.

In a study of citral hydrogenation on group VIII metals in different alcohols, Pak et al. reported dependencies on the H_2 pressure ranging from first order to a negative order [36]. For instance, a first-order reaction was reported for Pt black when ethanol was used as the solvent and P_{H_2} ranged from 20 to 80 atm, but a zero-order dependence on P_{H_2} was observed above 80 atm H_2. This change in reaction order, which appeared to occur at a certain limiting H_2 pressure that was dependent on the catalyst and the solvent, was associated with a possible change in reaction mechanism. The authors considered the possibility of weak citral adsorption occurring over semilayers of adsorbed hydrogen (at higher hydrogen pressures), with this citral subsequently undergoing hydrogenation [37]. The issues of rate dependence on the reactant concentrations and reaction modeling will be considered in detail in Part II of this series [17].

5. Conclusion

The overall effect of the solvent on the liquid-phase hydrogenation of citral on a Pt/SiO_2 catalyst was studied by comparing the reaction rate and product selectivity in eight different solvents: *n*-amyl acetate, ethyl acetate, *n*-hexane, cyclohexane, tetrahydrofuran, *p*-dioxane, ethanol, and cyclohexanol. These solvents had significantly different physical and electronic properties, and, based on spectroscopic results, they were nonreactive under the reaction conditions used. The catalyst was prepared using a Pt precursor containing no Cl to avoid possible contamination and to prevent side reactions leading to

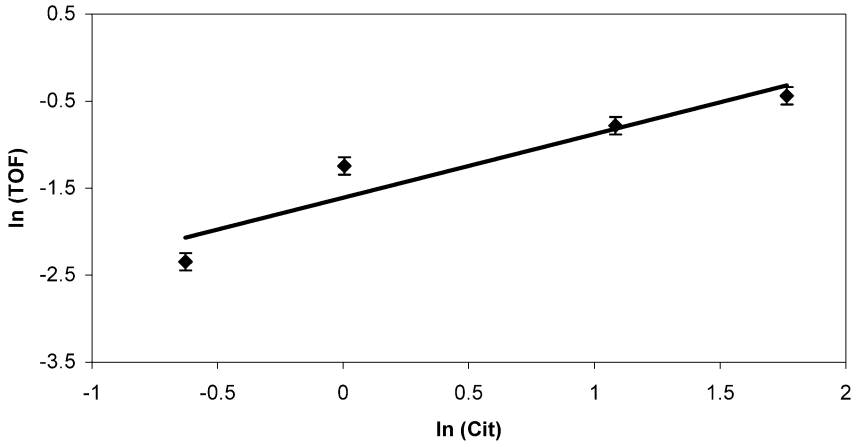

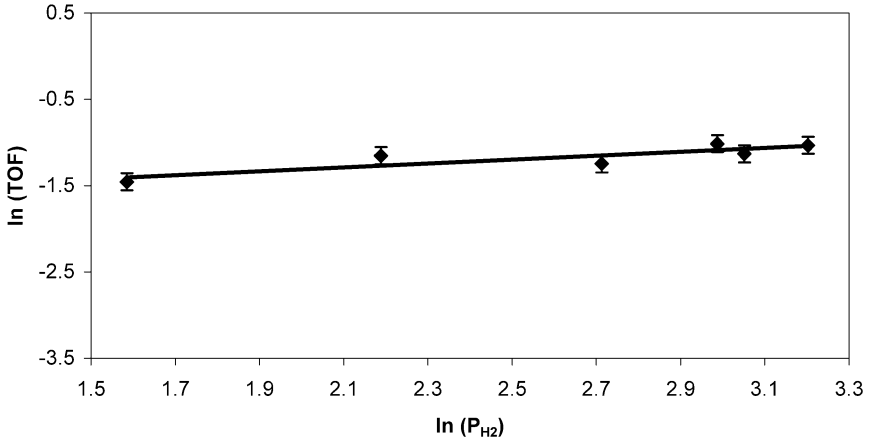

(c)

Fig. 5. (*continued*)

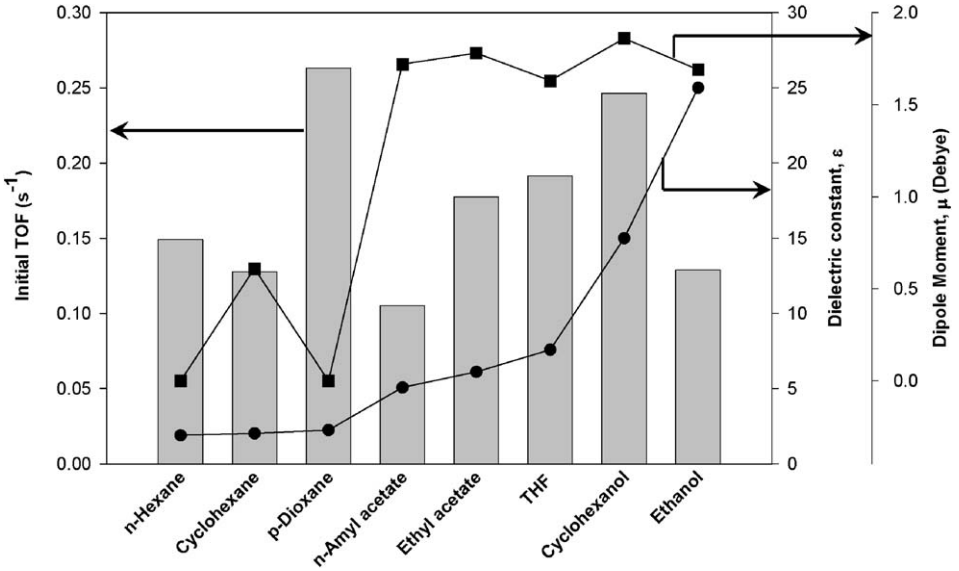

Fig. 6. Initial TOF (bars) for citral hydrogenation at 373 K (at 20 atm H_2, 1 M citral) plotted with the dielectric constant (●) and dipole moment (■) of each solvent. Dipole moment, μ (in gas), and dielectric constant, ε (at 293 K), values were taken from Ref. [16], while ε for *n*-amyl acetate (in gas) was obtained from Ref. [24].

acetal formation in the presence of alcoholic solvents. The reaction rate data, which were verified to be free of transport limitations, were compared both during the initial stage and after a 24-h period in the different solvents. The initial TOF showed

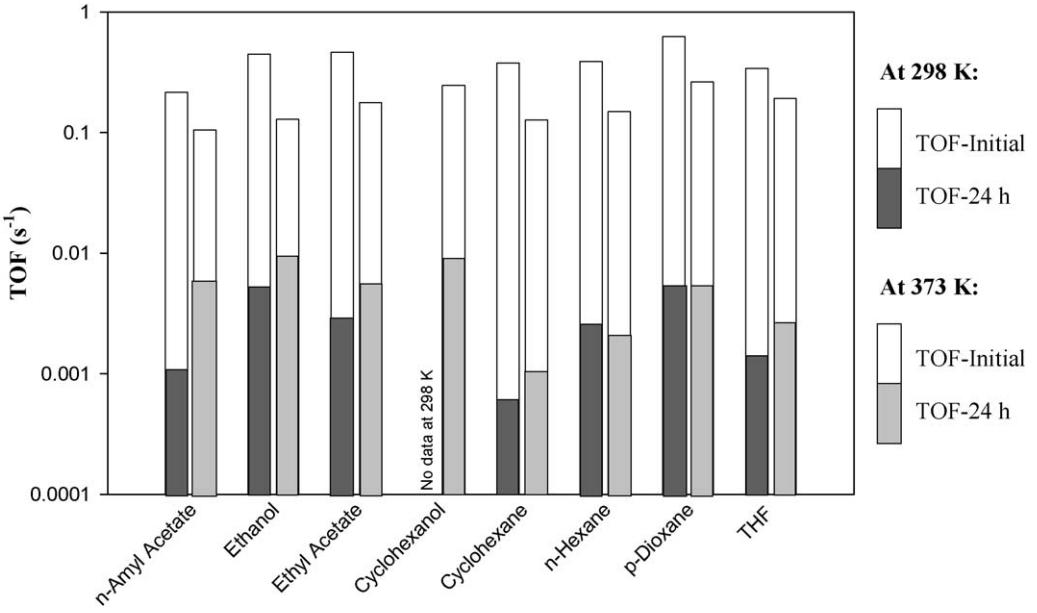

Fig. 7. Relative activities after 24 h of reaction in various solvents. Reaction conditions: 3.15% Pt/SiO_2, 20 atm H_2, and 1 M citral initially.

an approximately three-fold variation in different solvents at 298, 373, and 423 K, with the highest value always obtained in *p*-dioxane. This variation in specific activity did not correlate with either the solvent dielectric constant or the dipole moment, and the appropriateness of using either of these two solvent properties to explain solvent–solute interactions was discussed considering significant higher multipole moments that can be present in some nondipolar molecules such as *p*-dioxane and benzene.

These citral hydrogenation experiments showed that substantial catalyst deactivation occurred with increasing reaction time, presumably due to side reactions involving decarbonylation, presumably of the unsaturated alcohol. This deactivation decreased the TOFs by 1–2 orders of magnitude over a 24-h period, and it was more pronounced at 298 K than at 373 K. Although catalyst deactivation was noted in each solvent at 373 K, the total number of citral turnovers over a 24-h period was highest in ethanol and *p*-dioxane, double that of the lowest number obtained in cyclohexane and *n*-hexane. Very high citral conversions were obtained after 24 h at 423 K with cyclohexanol (96%) and ethanol (94%) under standard reaction conditions of 20 atm H_2 and 1 M citral.

In general, the solvent did not significantly influence the product distribution profiles for citral hydrogenation at these temperatures when compared at conversions near 30%, although selectivity to geraniol and nerol was always the lowest with *p*-dioxane at both 373 and 423 K, because sequential hydrogenation was enhanced. At these two temperatures, these two unsaturated alcohol stereoisomers usually composed around 70–80% of the product, but at 298 K, sequential hydrogenation reactions were favored, and much more citronellol and the final saturated dimethyloctanol product were produced. Low citral concentrations favor sequential hydrogenation reactions and thereby lower the selectivity to UALC; in contrast, the H_2 pressure did not impart any obvious general trends. In the eight solvents, the rate dependence on citral fell between one-half to first order, whereas the exponential dependence on H_2 pressure was relatively invariant at 0.3 ± 0.1.

Appendix A. Estimation of properties required to evaluate mass transfer limitations in liquids

A.1. Introduction

It is important to model the kinetics of heterogeneous catalytic reactions accurately using data free from heat and mass transfer effects so that valid rate expressions, which can include the influence of transport effects, can be derived for reactor design [18,38–40]. This can be challenging because of the complexities of reaction mechanisms and the physical structure characteristics of these heterogeneous catalytic systems; however, for liquid-phase reactions temperature gradients are usually not so important due to the relatively high values of heat capacity and thermal conductivity of the liquid phase compared to the vapor phase, so this facilitates the modeling. With a porous catalyst, diffusional limitations can alter the overall kinetics of a reaction via an external resistance (interphase transport between the fluid and solid phases) and an internal resistance (intraphase transport within the pore structure). There are established criteria and relatively easy experimental methods to determine the absence of external diffusion limitations; however, the assessment of pore diffusion limitations is more difficult because it depends on the catalyst as well as certain reaction parameters [14,41,42]. This appendix addresses the evaluation of diffusional limitations in porous catalysts in liquid-phase reactions, which is a topic that has had limited detailed attention in the catalysis literature. Although parts of this problem have been addressed by determining effective diffusivities in liquid-filled pores and evaluating mass transfer within small pores [43–45], there has been no systematic study on the role of solvents dur-

ing such assessments. To evaluate pore diffusion limitations in solvent-filled pores, existing criteria applicable to gas–solid reactions can be utilized after suitable modifications, and established methods exist to check for transport limitations in heterogeneous catalysts used for liquid-phase reactions. However, caution must be exercised when using any criterion that has not been specifically developed for a given catalyst–solvent system [46–52], and it is important to know the underlying assumptions of a particular criterion and its range of applicability. The objective here is to utilize a reasonably accurate analysis based on observable variables and measurable or calculable physical properties of the catalyst to readily determine the presence or absence of any significant internal mass transport limitations.

Hydrogenation of unsaturated aldehydes is an important class of reactions that yield intermediates useful in the fine chemical and pharmaceutical sectors. Kinetic studies in this area have concentrated on vapor-phase reactions [53–55], whereas nearly all of the liquid-phase hydrogenation investigations have focused on rate and selectivity characteristics and have seldom addressed issues such as solvent effects and transport effects on kinetic behavior [56]. This appendix examines the effect of the solvent on intraparticle diffusion in a porous catalyst used in a liquid-phase reaction. Procedures are referenced that allow one to estimate gas solubilities and the physical and thermodynamic properties required to calculate bulk diffusivities. Once these latter values are known, effective diffusivities within the pores can be calculated and a Weisz–Prater number (or a Thiele modulus) can be determined. A suitable approach to obtain a Weisz–Prater (WP) number is described, and it is then illustrated in detail using rate data for citral hydrogenation on a supported metal catalyst as an example.

A.2. Approaches to evaluate intraparticle diffusion effects

If the number of active sites can be quantified in a porous catalyst, including metal particles dispersed on a solid support, the Madon–Boudart method offers the best experimental approach to verify the absence of both mass and heat transfer limitations [14,18]. Its principal drawback is the need to vary and measure sites while keeping metal dispersion relatively constant with reactions that are structure-sensitive and therefore have specific activities that depend on crystallite size [14,38].

Alternatively, one traditional approach to determine diffusion resistance in a porous catalyst is the use of a Thiele modulus, which represents the ratio of the surface reaction rate to the diffusion rate of a reactant within the pores of a catalyst [57]. For a single species 'A' reacting within a porous medium to give an equimolar quantity of product via a simple nth-order rate expression of $r_A = k_n C_A^n$, a derivation of the Thiele modulus, ϕ, at steady state gives

$$\phi = \left[\frac{k_n (C_{s,A})^{n-1} S \rho R_p^2}{D_{eff}}\right]^{1/2}, \tag{A.1}$$

where, if k_n is expressed per unit surface area [with typical units],

$C_{s,A}$ = gas-phase concentration of 'A' at the particle surface [mol cm^{-3}],
k_n = rate constant of nth-order reaction [(mol$^{(1-n)}$ cm$^{(3n-2)}$)/s],
n = order of reaction,
S = internal surface area per unit mass of the catalyst [cm^2 g^{-1}],
ρ = density of the catalyst pellet [g cm^{-3}],
R_p = radius of the catalyst particle [cm],
D_{eff} = effective diffusivity of 'A' [cm^2 s^{-1}].

When the Thiele modulus is large, diffusion can control the overall rate of reaction and the observed rates are not representative of the true kinetics of the reaction. The internal effectiveness factor (the Thiele utilization factor) gives numerical values between 0 and 1 which indicate the relative importance of mass transport on the rate of reaction. This effectiveness factor, η, can be expressed as a function of a Thiele modulus for relatively high values of ϕ when diffusion control is occurring, i.e.,

$$\eta = \left(\frac{2}{n+1}\right)^{1/2} \frac{3}{\phi} = \left(\frac{2}{n+1}\right)^{1/2} \frac{3}{R_p} \sqrt{\frac{D_{eff}}{k_n S \rho} (C_{s,A})^{(n-1)}}. \tag{A.2}$$

The above expression for η assumes isothermal conditions, and a value close to unity indicates the absence of internal diffusion limitations [14,40,57,58]. The greatest difficulty with this approach is that the true rate constant, k_n, and the reaction order are frequently not known. In such cases, a reaction order must be assumed to allow k_n to be evaluated: for an example, see Ref. [14].

A third approach, which eliminates this difficulty, formulates the problem in a similar manner but requires only the observed (or measured) rate, r_A [47]. Based on this perspective, the Weisz–Prater criterion was derived [46,47], which again represents a ratio of the rate of reaction to the rate of diffusion in the pores and is stated as follows:

$$\phi_{WP} = \frac{r_a R_p^2}{C_{s,A} D_{eff}}, \tag{A.3}$$

where ϕ_{WP} is the dimensionless WP parameter and r_A is the observed rate per catalyst volume. Under isothermal reaction conditions, values of the WP criterion establishing the absence of significant internal mass transfer effects have been summarized in Table A.1. A value for $\phi_{WP} > 6$ indicates definite diffusional control [47], whereas a value less than 0.3 can be considered a sufficient condition for the absence of significant pore diffusion limitations because few reactions have a reaction order greater than two. However, in reactions involving strong product inhibition, the observed reaction rate can be much lower than in an uninhibited reaction, thereby yielding a smaller ϕ_{WP} value, as

Table A.1
Weisz–Prater criteria for different reaction orders

Effectiveness factor	Reaction order	Value of ϕ_{WP}
$\eta \geqslant 0.95$	$n = 0$	$\phi_{WP} \leqslant 6$
$\eta \geqslant 0.95$	$n = 1$	$\phi_{WP} \leqslant 0.6$
$\eta \geqslant 0.95$	$n = 2$	$\phi_{WP} \leqslant 0.3$

shown by Peterson who also points out that the WP criterion can be modified to address this complication and still be used in a valid fashion [49].

To use the WP criterion (or a Thiele modulus) successfully, one must accurately determine the effective diffusivity of a reactant in a given catalyst system. This is easily done in the gas (or vapor) phase by comparing the mean free path (λ) with the average pore diameter ($\bar{d}$) to determine which parameter controls the effective diffusivity. If it is the latter, Knudsen diffusion dominates and to a good approximation $D_{\text{eff}} \cong D_{\text{Kn}} = 1/3\bar{v}\bar{d}$, where $\bar{v}$ is the average molecular velocity. For liquid-phase reactions, the catalyst pores are filled primarily with solvent, if one is used, and the molecular diffusivity of the solute (the reactant) can be several orders of magnitude lower in a liquid-phase system compared to a vapor-phase system. Apart from a decrease in bulk diffusivity, there can also be liquid-phase non-idealities, adsorption phenomena, and other factors influencing the effective diffusivity [59]. If the size of the diffusing molecules is comparable to the pore size, diffusion in the pores is hindered [43,60–62]. A different situation arises when the diffusing species has a high affinity for the catalytic surface, which can lead to surface diffusion and migration [40, 63]; however, this contribution may be important only in certain low-temperature vapor-phase reactions [64].

A.3. Application of the WP criterion to liquid-phase reactions

Regarding the effective diffusivity, it might be borne in mind that the objective of this appendix is to determine a reasonable value of the WP criterion based on the important characteristics of the system. Such a calculation should establish the absence of any pore diffusion limitations or warn of their presence. As stated earlier, a good rule for the absence of significant diffusion limitations is a value of ϕ_{WP} below 0.3. Let us now examine briefly the quantities involved in evaluating the WP criterion with respect to liquid-phase reactions.

The rate, r_A, in ϕ_{WP} (Eq. (A.3)) is experimentally measured under a given set of reaction conditions. The concentration of a reactant 'A' at the surface of the catalyst, $C_{s,A}$, can be assumed to be equal to the bulk concentration, C_A, if external mass transfer limitations have been removed by appropriate mixing. Thus the bulk-phase concentration can be used even though it could give a ϕ_{WP} value somewhat smaller than the actual value. The size of the catalyst particles can be determined independently to get the particle radius, R_{p}. Consequently, the effective diffusivity, D_{eff}, is the most difficult to evaluate because it will depend not only on the relative sizes of the diffusing molecule and the pores, but also on the bulk diffusivity in the liquid reactant (if pure) or the reactant–solvent mixture. Although surface diffusion may occur in some vapor-phase systems [64], it can be neglected in a liquid-phase system and, moreover, its exclusion would only yield a slightly lower estimate of D_{eff} and provide an upper limit for the WP criterion.

To assess hindered diffusion of a species through a pore structure, appropriate pore size data are required. The average pore size, characterized by a pore radius, r_{p}, is not an issue with catalysts having relatively uniform pores. If a pore size distribution exists, a mean pore radius can be estimated using the internal specific surface area, S, the bulk density of the catalyst pellet, ρ, and the catalyst porosity (i.e., the void fraction), ε, as shown below [40,63]:

$$\bar{r}_{\text{p}} = \frac{2\varepsilon}{S\rho}. \tag{A.4}$$

A pelletized or extruded catalyst prepared by compacting fine powder particles typically exhibits a bimodal (macro–micro) pore size distribution, in which case the mean pore radius is probably an inappropriate representation of the pore size. There are several analyses and models in the literature to represent pelletized catalysts, but they involve complicated diffusion equations and may require the knowledge of diffusion coefficients and void fractions for micro- and macropores [65]. An easier and more pragmatic approach is to consider the dimensional properties of the fine particles constituting the pellet and use the average pore size of only the micropore system because diffusional resistances will be significantly higher in micropores than in macropores. This will tend to underestimate D_{eff} values and again provide an upper limit for the WP criterion.

A.4. Obtaining D_{eff} values for liquid-phase systems

The topic of solute diffusivity in liquid-filled pores has been addressed and modifications to the conventional model for diffusivity have been provided by incorporating empirical constants, as shown below [43,62]:

$$D_{\text{eff}} = D_{\text{b}} \frac{\varepsilon}{\tau} \left\{ A \exp(-B\lambda)t \right\}. \tag{A.5}$$

Here, D_{b} is the diffusivity in the bulk phase, ε and τ are the catalyst porosity and tortuosity, respectively, λ is the ratio of the radius of the diffusing molecule to the pore radius (i.e., $r_{\text{molecule}}/r_{\text{pore}}$), and A and B are empirical constants based on the catalyst and the type of diffusing molecule. The possibility of hindered diffusion with molecules diffusing through micropores of similar dimensions cannot be overlooked. Ternan, in his treatment of diffusion of solute molecules in liquid-filled pores, developed an expression for effective diffusivity involving only one empirical constant for a given material:

$$D_{\text{eff}} = D_{\text{b}} \frac{(1-\lambda)^2}{1+P\lambda}, \tag{A.6}$$

in which the empirical constant, P, is a fitting parameter obtained from diffusivity data for various solutes diffusing through solvent-filled pores of that catalyst [66]. After making an appropriate choice of an expression to evaluate effective diffusivity of the reacting species in a specific liquid-phase system, determination of the bulk diffusivity is an important task and, unless D_{b} values are available from the literature for the particular solute–solvent system at reaction conditions, they have to be estimated from standard formulations based on physical properties of the solute (reactant) and the solvent. Depending on whether the solute is a gas or a liquid, a suitable expression for diffusivity must be chosen, and some of the common situations and the corresponding expressions to evaluate diffusivity

Table A.2a
Equations to calculate bulk diffusivities

(a) Diffusivity of a dilute gas solute in a liquid solvent [68]:

$$D_{12}^0 = 1.1728 \times 10^{-16} \frac{T\sqrt{\chi M_2}}{\eta_2 V_1^{0.6}}. \quad \text{(A.7)}$$

(b) Diffusivity of a dilute solute (<10 mol%) in water [69]:

$$D_{12}^0 = \frac{8.621 \times 10^{-14}}{\eta_2^{1.14} V_1^{0.589}}. \quad \text{(A.8)}$$

(c) Diffusivity of a dilute solute (<10 mol%) in any solvent except water [70]:

$$D_{12}^0 = 4.4 \times 10^{-15} \frac{T}{\eta_2} \left(\frac{V_2}{V_1}\right)^{1/6} \left(\frac{L_2^{\text{vap}}}{L_1^{\text{vap}}}\right)^{1/2}. \quad \text{(A.9)}$$

(d) Diffusivity in concentrated binary liquid systems using activity coefficient parameters [71]:

$$D_{12} = (x_1 D_{21}^0 + x_2 D_{12}^0)\alpha_{12}. \quad \text{(A.10)}$$

(e) Diffusivity in concentrated binary liquid systems using viscosity data [72]:

$$D_{12} = \frac{(D_{21}^0 \eta_1)^{x_1} (D_{12}^0 \eta_2)^{x_2}}{\eta_m}. \quad \text{(A.11)}$$

(f) Diffusivity of a solute in a mixture of two solvents [73]:

$$\ln(D_{1m}\eta_m^{0.5}) = x_2 \ln(D_{12}^0 \eta_2^{0.5}) + x_3 \ln(D_{13}^0 \eta_3^{0.5}). \quad \text{(A.12)}$$

Table A.2b
Definition of terms

Term	Definition
D_{ij}^0	Diffusivity at infinite dilution of i in j [$\text{cm}^2\,\text{s}^{-1}$]
D_{ij}	Diffusivity of i in the concentrated binary mixture [$\text{cm}^2\,\text{s}^{-1}$]
T	System temperature [K]
χ	Solvent association parameter
M_i	Molecular weight of component i
η_i	Viscosity of component i [Pa s]
x_i	Mole fraction of component i
V_i	Molar volume of component i at normal boiling point [m^3/kmol]
L_i^{vap}	Enthalpy of vaporization of component i at normal boiling point [J kmol^{-1}]
α_{12}	Thermodynamic correction term [$\alpha_{12} = 1 + d(\ln\gamma_1)/d(\ln x_1)$]
γ_i	Activity coefficient of component i
Subscripts	
1	Solute
2, 3	Solvents
m	Mixture

in liquid systems are listed in Table A.2a along with necessary definitions (Table A.2b) [67].

The reaction under consideration may involve a solvent and/or one or more liquid-phase products, thus making it a multi-component diffusion system. In such cases, D_b represents the solute diffusivity in the liquid mixture rather than a pure liquid, and a meaningful estimate of D_b can be obtained by neglecting relatively insignificant components. Equation (A.12) in Table A.2a can be used to calculate the diffusivity of a solute, gas or liquid, in a mixture of two liquid solvents.

A.5. Evaluating the WP criterion for liquid-phase citral hydrogenation

Hydrogenation of citral provides a complex reaction network involving 6–8 important intermediates [5,8,19,32,35,74]. The reaction chemistry during hydrogenation of the two stereoisomers of citral includes a number of series-parallel reactions, each of which represents the addition of one mole of dihydrogen [17]. Although the WP criteria was originally derived for a less complicated catalytic reaction, it can still be applied to this type of reaction scheme by examining the relative diffusivity of each reactant (citral and hydrogen) in the liquid-filled pores. However, the reactant with the lower effective diffusivity cannot be automatically assumed to be the more likely diffusion-controlling species because the liquid-phase concentration (the driving force) and the relative rate of consumption are also included in the WP parameter. The rate data used in this example were obtained from citral hydrogenation runs at 20 atm pressure and 373 K in various solvents using a silica-supported Pt catalyst [17].

Singh and Vannice verified the absence of external and internal mass transfer limitations during hydrogenation in the citral/*n*-hexane system using the Madon–Boudart technique as well as the WP criterion [5,8]. Supported Pt and Pd catalysts were prepared with widely varying concentrations of active sites (surface Pt or Pd atoms) but with similar metal dispersions in case these reactions were structure sensitive. The data here include the same reaction on a Pt/SiO_2 catalyst carried out in seven additional solvents.

The rate of reaction based on citral disappearance decreases because the reaction is carried out in a batch mode relative to citral and the citral concentration drops as the reaction proceeds. This aspect coupled with product formation changes the composition of the liquid inside the pores, which could alter the effective diffusivity. Such issues within the reaction system must be considered and an appropriate choice to model intraparticle diffusion must be made so that a meaningful WP value is obtained. The initial (or highest) rate of reaction and the initial citral concentration are chosen for r_A and $C_{s,A}$, respectively. Dihydrogen is fed continuously to maintain a constant H_2 pressure, so in a well-mixed system with no gas–liquid transport limitations the H_2 molecules in the two phases can be assumed to be quasi-equilibrated and Henry's law can be applied to determine the H_2 concentration in the liquid phase.

As discussed later, some of the physical properties of citral must be estimated using group-contribution methods (GCM) or other thermodynamic correlations due to their unavailability in the literature. The conversion of citral as the reaction progresses will change the composition of the liquid in the pores, but the intermediate products of this hydrogenation reaction are similar to citral in molecular size and configuration, so they will be assumed to have similar physical properties. Moreover, the typical concentration of citral in these runs is less than 10 mol%, and the products will exist in even smaller concentrations, so the physical properties of the initial liquid phase should not change significantly during the course of the reaction and the effective diffusivity calculated at initial reaction conditions should

Table A.3
Catalyst properties

Catalyst	3% Pt/SiO_2
Preparation	Ion-exchange method
Pretreatment	Reduced in situ in flowing H_2 at 673 K for 75 min
Metallic dispersion	$Pt_s/Pt_{total} = 1.0$
Particle radius	$R_p = 50$ μm
Pore radius[a]	$r_p = 7$ nm
Particle density[a]	$\rho_p = 0.4$ g/cm^3

[a] For Grade 57 Grace-Davison silica.

Table A.4
Operating conditions and reaction parameters

Temperature	373 K
Pressure	20 atm
Citral concentration	1 mol/L
Agitation	1000 rpm
Total liquid volume	60 cm^3
Solvents used	*n*-Amyl acetate, ethanol, ethyl acetate, cyclohexanol, cyclohexane, *n*-hexane, *p*-dioxane, tetrahydrofuran (THF)

be relatively invariant. Consequently, it should be sufficient to calculate the WP criterion once, based on the initial reaction conditions, to obtain a satisfactory estimate of the influence of intraparticle (pore) diffusion on this hydrogenation reaction. If the WP criterion gives a non-definitive value in the borderline region (between 0.3 and 6), additional calculations can be performed using reactant concentrations and rates taken at different reaction times [75]. The properties of the catalyst and the operating conditions used for this reaction are given in Tables A.3 and A.4, respectively, and the initial reaction rate data can be found in Table 1 of the main text.

The most important quantity that needs to be evaluated is the effective diffusivity. Because there are two diffusing reactants in this system, namely citral and H_2, it is necessary to compute the diffusivity of each in the liquid-filled pores. As mentioned previously, Ternan has derived an expression for D_{eff} based only on λ ($= r_{molecule}/r_{pore}$) and a single fitting parameter, and he incorporated two correction factors—one for a concentration effect and one for a pore wall effect. The former was addressed by assuming that the pore cross-sectional area near the pore wall corresponding to $r_{pore} - r_{molecule}$ was unavailable to solute molecules, but smaller solvent molecules could be present in this excluded region, thus causing a lower solute concentration in the pore compared to that outside the pore in the bulk liquid. The latter correction for a 'pore wall effect' considered a viscosity variation near the pore wall caused by its force field. The significance of a change in viscosity, η, is reflected by the Stokes–Einstein equation, i.e.,

$$\frac{D\eta}{T} = \text{constant}. \tag{A.13}$$

The final form of the effective diffusivity expression derived by Ternan is

$$D_{eff} = D_b \frac{(1-\lambda)^2}{1+P\lambda}. \tag{A.14}$$

The fitting parameter, P, for a silica–alumina catalyst was calculated by Ternan to be 16.3 based on data reported by Satterfield et al. [62]. In the absence of diffusivity data for the silica used in this study, this value of P was utilized to compute effective diffusivities. From Eq. (A.14) it is clear that one solvent effect manifests itself through the D_b values.

A.6. An example: Calculating the WP criterion with ethanol as the solvent

In this section, a detailed evaluation will be presented with ethanol (EtOH) as the solvent. Let us first consider dihydrogen as the diffusing component. The diffusivity of H_2 in either citral or the solvent can be estimated from the method of Wilke and Chang [68], i.e., Eq. (A.7) in Table A.2a:

$$D_{H_2/solv}\ (\text{m}^2\,\text{s}^{-1}) = 1.1728 \times 10^{-16} \frac{T\sqrt{\chi_{solv} M_{solv}}}{\eta_{solv} V_{H_2}^{0.6}}. \tag{A.15}$$

Care must be taken to use consistent units for the quantities involved, and the constants used in the above equation give units of m^2 s^{-1} for diffusivity. The properties of the solvents used in the calculations are given in Table A.5. The molar volume of H_2 at its normal boiling point is $V_{H_2} = 0.0286$ m^3 kmol^{-1} [76]. It should be noted that the concentration of hydrogen in the liquid phase is on the order of 0.1 mmol cm^{-3}; therefore, H_2 may be neglected as a constituent in the bulk phase for all volumetric purposes. At the reaction temperature ($T = 373$ K), the diffusivity of H_2 in citral and ethanol is calculated from Eq. (A.15) to be 1.08×10^{-4} and 9.23×10^{-5} cm^2 s^{-1}, respectively. Now the effective binary diffusion coefficient of H_2 in the mixture can be computed using Eq. (A.12) in Table A.2a, i.e.,

$$D_{H_2/mixt} = \frac{(D_{H_2/citral}\eta_{citral}^{0.5})^{x_{citral}} (D_{H_2/EtOH}\eta_{EtOH}^{0.5})^{x_{EtOH}}}{\eta_{mixt}^{0.5}}. \tag{A.16}$$

Further, the viscosity of the mixture required in Eq. (A.16) may be computed as [67]

$$\eta_{mixt} = \eta_{citral}^{x_{citral}} \eta_{EtOH}^{x_{EtOH}}. \tag{A.17}$$

A value of 9.3×10^{-5} cm^2 s^{-1} was thereby obtained for the diffusivity of H_2 in the mixture, which is close to the diffusivity of H_2 in EtOH because of the small mole fraction of citral ($x_{citral} = 0.068$).

Although catalytic studies have encompassed a wide variety of organic compounds and many different types of reactions, obtaining physical properties for uncommon chemicals is a challenge. Citral is such a molecule and information about it is scarce but, fortunately, there are methods available to estimate thermodynamic properties [67,77–82]. The data prediction manual compiled by Danner and Daubert is extremely useful for the estimation of diffusivity and thermal or physical properties of compounds in the absence of experimental data [67]. In the present study a number of properties for citral had to be estimated, such as the critical temperature (T_c), critical pressure (P_c), saturated density (ρ_{sat}), viscosity (η), enthalpy of vaporization (L^{vap}), and solubility parameter (δ), and

Table A.5
Physical properties of the solvents [15]

Solvent	Mol. wt.	V_i at T_b[a] ($m^3\,kmol^{-1}$)	χ[b]	L_i^{vap} at T_b[a] ($J\,kmol^{-1} \times 10^{-7}$)	η_i at 373 K ($Pa\,s \times 10^4$)	H_{H_2}[c] (atm)	C_{s,H_2}[d] ($mol\,cm^{-3} \times 10^5$)
n-Amyl acetate	130	0.175	1.0	3.85	3.57	1360	9.48
Ethanol (EtOH)	46	0.0626	1.5	3.94	3.32	3420	9.09
Ethyl acetate	88	0.106	1.0	3.22	2.12	1490	12.2
Cyclohexanol	100	0.123	1.0	4.59	20.2	2690	7.03
Cyclohexane	84	0.117	1.0	2.99	3.05	1800	9.06
n-Hexane	86	0.140	1.0	2.91	1.58	1040	14.0
p-Dioxane	88	0.0938	1.0	3.43	3.90	3160	6.94
THF	72	0.0863	1.0	3.03	2.34	1970	10.0

[a] T_b: Normal boiling point.
[b] χ: Association parameter, see Ref. [67].
[c] Henry's law constant at 373 K, see Ref. [12].
[d] At 373 K, 20 atm total pressure, and 1 M citral, see Ref. [12].

Table A.6
Calculated physical and thermodynamic properties of citral

Property	Calculated value	References
Critical temperature, T_c	699 K	[12,77,78]
Critical pressure, P_c	22.6 atm	[12,77,78]
Saturated density, ρ_{sat}	$0.827\,g\,cm^{-3}$[a]	[12,79]
Molar volume at B.P., V_{citral}	$0.171\,m^3\,kmol^{-1}$[b]	[12]
Viscosity, η	$4.22 \times 10^{-4}\,Pa\,s$[a]	[12,67,80]
Vaporization enthalpy, L^{vap}	$4.41 \times 10^7\,J\,kmol^{-1}$[b]	[12,67,81]
Solubility parameter, δ	$18.3\,J^{0.5}\,cm^{-1.5}$[c]	[12,82]
Henry's law constant, H_{H_2}	1310 atm[a]	[12]

[a] At $T = 373$ K.
[b] At normal boiling point, $T_b = 501$ K.
[c] At $T = 298$ K.

these values are listed in Table A.6 along with the procedures used for estimation. Details of these calculations are provided elsewhere [12]. The values for the H_2 concentration at the particle surface given in Table A.5 are those for the H_2 solubility in the liquid mixture at the stated conditions based on Henry's law constants for H_2 in citral and the respective solvents. These Henry's law constants were either obtained from solubility data reported in the literature or computed using thermodynamic techniques involving the Soave–Redlich–Kwong (SRK) equation of state [83–85]. The latter approach gave values in good agreement with experimental data, when available for comparison [12].

In the next part of this analysis, citral is considered to be the diffusing component. To estimate the binary diffusivity of citral in EtOH, Eq. (A.9) in Table A.2a can be used:

$$D_{citral/mixt} = D_{citral/EtOH}\ (m^2\,s^{-1}) = 4.4 \times 10^{-15} \frac{T}{\eta_{EtOH}} \left(\frac{V_{EtOH}}{V_{citral}}\right)^{1/6} \left(\frac{L_{EtOH}^{vap}}{L_{citral}^{vap}}\right)^{1/2}. \quad (A.18)$$

The values for the molar liquid volume for different solvents at their normal boiling point were determined based on a modified form of the Rackett equation, which correlates the saturated liquid density as a function of temperature [15]:

$$\rho_{liq}^{sat} = A B^{-(1-T/T_c)^n}, \quad (A.19)$$

Table A.7
Effective diffusivities of citral and hydrogen in EtOH at 373 K

Component	$r_{molecule}$ (nm)	$\lambda = \frac{r_{molecule}}{r_{pore}}$	D_b ($cm^2\,s^{-1} \times 10^5$)	D_{eff} ($cm^2\,s^{-1} \times 10^5$)
Citral	0.39	0.056	3.80	1.78
Hydrogen	0.12	0.017	9.33	7.05

where A, B, and n are regression coefficients for a given liquid, and T_c is the critical temperature. With the properties given in Table A.5, the value of $D_{citral/mixt}$ turns out to be $3.8 \times 10^{-5}\,cm^2\,s^{-1}$. With these two values for the bulk diffusivity of H_2 and citral in the reaction mixture and the λ values in Table A.7, the effective diffusivity of each reactant in the catalyst pores was computed using Eq. (A.14), and the D_{eff} values are also listed in Table A.7. These latter values are significantly lower than the respective bulk diffusivities and demonstrate the need to correct for hindered diffusion in the pores, even for H_2.

Although the effective diffusivity for H_2 in the pores is more than four times greater than that for citral, it cannot be automatically inferred that the latter molecule is more likely to control the rate due to pore diffusion. This is because the reactant concentration (the driving force for diffusion) as well as its rate of consumption is contained in ϕ_{WP}. Consequently, with the values in Tables A.3, A.5, and A.7, application of the WP criterion for each reactant gives

$$\phi_{WP|H_2} = \frac{(8.4 \times 10^{-6}\ \frac{mol}{cm^3\,s})(5.0 \times 10^{-3}\ cm)^2}{(9.09 \times 10^{-5}\ \frac{mol}{cm^3})(7.05 \times 10^{-5}\ \frac{cm^2}{s})} = 0.03 < 0.3 \quad (A.20)$$

and

$$\phi_{WP|citral} = \frac{(8.4 \times 10^{-6}\ \frac{mol}{cm^3\,s})(5.0 \times 10^{-3}\ cm)^2}{(1 \times 10^{-3}\ \frac{mol}{cm^3})(1.78 \times 10^{-5}\ \frac{cm^2}{s})} = 0.01 < 0.3. \quad (A.21)$$

The value of ϕ_{WP} for each reactant is more than an order of magnitude less than 0.3, which assures the absence of significant pore diffusional limitations during citral hydrogenation in EtOH under these conditions. Surprisingly, the ϕ_{WP} value for hydrogen is greater than that for citral, and indicates that H_2 diffusion, rather than citral diffusion, is more likely to inhibit the reaction rate. In the previous calculations the same reaction

Table A.8
Evaluation of the WP criterion for citral hydrogenation in different solvents

Solvent	Rate (μmol s^{-1} g$_{cat}^{-1}$)	Diffusivity values (cm^2 s^{-1} $\times$ 10^5)				η_m (Pa s $\times$ 10^4)	$\phi_{WP\|H_2}$	$\phi_{WP\|citral}$
		$D_{b,H_2\|mix}$	$D_{b,citral\|mix}$	D_{eff,H_2}	$D_{eff,citral}$			
n-Amyl acetate	7.1	11.6	4.15	8.79	1.94	3.66	0.02	0.01
Ethanol	8.4	9.33	3.80	7.05	1.78	3.37	0.03	0.01
Ethyl acetate	11.6	15.6	5.88	11.8	2.75	2.29	0.02	0.01
Cyclohexanol	16.1	2.24	0.75	1.69	0.35	16.9	0.3	0.1
Cyclohexane	8.4	11.1	4.00	8.36	1.87	3.17	0.03	0.01
n-Hexane	9.7	19.7	7.86	14.9	3.67	1.81	0.01	0.01
p-Dioxane	16.8	9.04	3.23	6.83	1.51	3.93	0.09	0.03
THF	12.3	13.2	4.99	9.94	2.33	2.46	0.03	0.01

Note. Reaction conditions: 1 M citral, 373 K, and 20 atm.

rate was used for both dihydrogen and citral, which is justified because the initial (i.e., maximum) rate of reaction involves the conversion of citral to geraniol, nerol or citronellol, with each reaction consuming equimolar amounts of H_2 and citral. If significant secondary reactions occurred to form intermediate products like citronellol and 3,7-dimethyloctanol within the first sampling time period, the molar rate of hydrogen consumption would exceed that of citral, which would increase the ϕ_{WP} value for H_2 and further accentuate the possibility that H_2 transport in the pores is more likely to induce diffusional limitations on the rate.

A.7. Effect of different solvents on ϕ_{WP} values

The diffusivities and WP criterion values calculated for different solvents in the same manner as for EtOH are presented in Table A.8. The results verify the absence of any significant internal mass transfer limitations ($\phi_{WP} \leqslant 0.3$) with any of these solvents under the stated reaction conditions, and the ϕ_{WP} values for H_2 are greater than or equal to these for citral. The ϕ_{WP} value for a particular solvent depends on a number of factors in a complex way. For instance, an increase in temperature decreases viscosity and thus increases the diffusivity, but it concurrently decreases C_{s,H_2}, the solubility of H_2 in the mixture. Among the different solvents, the value of $\phi_{WP|H_2}$ correlates strongly with the viscosity of the reaction medium (η_{mixt}) [12], as seen from the results in Table A.8. The cyclohexanol–citral mixture with the highest viscosity also exhibits the largest WP numbers. The results in Table A.8 were computed based on a specific set of reaction conditions, and H_2 need not be the more likely diffusion-limiting reactant because a higher H_2 partial pressure increases the value of C_{s,H_2} and decreases $\phi_{WP|H_2}$; consequently, just by the choice of H_2 pressure and/or temperature one can move the reaction from a regime of kinetic control to one of H_2 mass transfer control.

By using a value of 0.3 for ϕ_{WP}, a guideline can be established to determine reaction parameters giving either the maximum allowable rate or the maximum allowable particle size before the onset of diffusional limitations. Furthermore, if the apparent activation energy is known, ϕ_{WP} can be plotted versus temperature to establish temperature regimes in which both, one, or neither reactant satisfies the WP criterion for kinetic control [12]. Colen et al. evaluated the effects of pore diffusion on the hydrogenation rate of triacylglycerol to tristearoylglycerol on a supported Ni catalyst using a Thiele modulus, and they observed that increasing the hydrogen pressure could increase the rate enough so that pore diffusion became significant [75]. Consequently, such calculations can be very useful in optimizing a reactor design.

A.8. WP analysis of hydrogenation data from the literature

An adequate analysis of the pore diffusion limitations within heterogeneous catalysts can allow one to either ascertain a kinetic regime or deliberately operate in a mass-transfer-controlled regime. The latter situation may be significant from an industrial viewpoint where altering selectivity or controlling the reaction rate (and its exothermicity) is critical. In a research environment, where the focus is typically on investigating the kinetic behavior of the reaction network, it is imperative to generate data that are free of transport limitations. Literature studies of liquid-phase hydrogenation reactions were reviewed and a WP analysis was performed whenever sufficient information was available [12]. For simplicity, only catalyst systems using a silica support were considered, and two such cases will be considered for a detailed WP analysis.

A review paper by Cerveny and Ruzicka on competitive liquid-phase hydrogenation reactions provides *individual* rate data for a number of olefinic substrates in a wide variety of solvents [86]. For example, the hydrogenation rates of 1-hexene on a 5% Pt/SiO_2 catalyst in 17 different solvents varied by two orders of magnitude depending on the solvent [87]. The silica support used in their study had an average pore radius of 4 nm, a total pore volume in the range of 0.60 to 0.75 cm^3 g^{-1}, and the grain size was reported as being <63 μm [88]. Assuming a catalyst porosity of 0.5, the bulk density of the catalyst was estimated to be 0.74 g cm^{-3} [12]. The rate data at 293 K, given in terms of ml H_2/min/g_{cat} (corrected to a H_2 partial pressure of 1 atm), were converted to suitable WP units using this catalyst density. Needed physical and thermodynamic properties for solvents not discussed in the present study along with H_2 solubilities were evaluated by the methods described earlier, and they are listed elsewhere [12]. Using a particle radius of 31.5 μm to calculate WP numbers [12], $\phi_{WP|hexene}$ values varied from 0.02 to 1.8 while $\phi_{WP|H_2}$ values ranged from 0.7 to 205 with 13 solvents having values of 6 or greater, which indicates a diffusion-controlled regime [14,46,47]. Consequently,

the use of this low H_2 pressure (1 atm) resulted in rate data affected by H_2 mass transfer limitations and some runs may have also suffered from hexene diffusional effects.

The second case is a study by Hajek and Murzin of cinnamaldehyde hydrogenation on a Ru–Sn/SiO_2 sol–gel catalyst [89]. Here the authors specifically investigated the effect of different mass transfer resistances using a combined theoretical/experimental approach. The catalyst in their study had a narrow pore distribution between 1 and 4 nm and a bulk density of 0.75 $g\,cm^{-3}$. The cinnamaldehyde hydrogenation reaction was carried out in 2-propanol at 433 K and 69.1 atm total pressure (58.2 atm H_2 partial pressure). A reaction rate of 12.3×10^{-4} $mol/min/g_{cat}$ was obtained using a catalyst with a mean particle size of 23 μm. Using a H_2 solubility in 2-propanol of 3.2×10^{-4} $mol\,cm^{-3}$ and a D_{eff} value of 8.7×10^{-5} $cm^2\,s^{-1}$ at these conditions [90] and an average pore diameter of 2 nm, the ϕ_{WP} value with respect to H_2 was 0.044, which verifies the absence of H_2 transport limitations, in agreement with the author's analysis using a Thiele modulus [89]. However, the possibility of cinnamaldehyde diffusion limitations was not addressed. Their cinnamaldehyde concentration in the solvent was below 1 mol%, and a D_{eff} value of 8.6×10^{-6} $cm^2\,s^{-1}$ was estimated for the given reaction conditions, which gave a WP number of 1.3 for 2 nm pores and 0.66 for 3 nm pores [12]. Thus, although borderline, there is a possibility that some mass transfer effects may have existed with cinnamaldehyde.

References

[1] L. Mercadante, G. Neri, C. Milone, A. Donato, S. Galvagno, J. Mol. Catal. 105 (1996) 93.
[2] P. Gallezot, D. Richard, Catal. Rev. Sci. Eng. 40 (1998) 81.
[3] M. Englisch, V.S. Ranade, J.A. Lercher, Appl. Catal. A Gen. 63 (1997) 111.
[4] M. Englisch, V.S. Ranade, J.A. Lercher, J. Mol. Catal. A Chem. 121 (1997) 69.
[5] U.K. Singh, M.A. Vannice, J. Catal. 191 (2000) 165.
[6] U.K. Singh, M.N. Sysak, M.A. Vannice, J. Catal. 191 (2000) 181.
[7] U.K. Singh, M.A. Vannice, J. Mol. Catal. A Chem. 163 (2000) 233.
[8] U.K. Singh, M.A. Vannice, J. Catal. 199 (2001) 73.
[9] J. Kijenski, P. Winiarck, Appl. Catal. A Gen. 193 (2000) L1.
[10] F. Iosif, S. Coman, V. Parvulescu, P. Grange, S. Delsarte, D. De Vos, P. Jacobs, Chem. Commun. 11 (2004) 1292.
[11] A.F. Trasarti, A.J. Marchi, C.R. Apesteguia, J. Catal. 224 (2004) 484.
[12] S. Mukherjee, Ph.D. thesis, Pennsylvania State University, University Park, 2005.
[13] M.B. Palmer, M.A. Vannice, J. Chem. Technol. Biotechnol. 30 (1980) 205.
[14] M.A. Vannice, Kinetics of Catalytic Reactions, Springer–Kluwer, New York, 2005, Chap. 4.
[15] C.L. Yaws, Chemical Properties Handbook: Physical, Thermodynamic, Environmental, Transport, Safety, and Health Related Properties for Organic and Inorganic Chemicals, McGraw–Hill Handbooks, McGraw–Hill, New York, 1999.
[16] R.H. Perry, D.W. Green (Eds.), Perry's Chemical Engineers' Handbook, seventh ed., McGraw–Hill Professional, New York, 1997.
[17] S. Mukherjee, M.A. Vannice, J. Catal. 243 (2006) 108, this issue.
[18] R.J. Madon, M. Boudart, Ind. Eng. Chem. Fund. 21 (1982) 438.
[19] M.A. Aramendia, V. Borau, C. Jimenez, J.M. Marinas, A. Porras, F. Urbano, J. Catal. 172 (1997) 46.
[20] G. Neri, L. Mercadante, A. Donator, A.M. Visco, S. Galvagno, Catal. Lett. 29 (1994) 379.
[21] J.H. Sinfelt, H. Hurwitz, J.C. Rohrer, J. Phys. Chem. 64 (1960) 892.
[22] F.G. Ciapetta, J.B. Hunter, Collect. Czech. Chem. Commun. 45 (1953) 147.
[23] R.A. Rajadhyaksha, S.L. Karwa, Chem. Eng. Sci. 41 (1986) 1765.
[24] A.L. McClellan, Tables of Experimental Dipole Moments, vol. 1, Freeman, San Francisco, 1963.
[25] C. Reichardt, Solvents and Solvent Effects in Organic Chemistry, Wiley–VCH, Weinheim, 2003.
[26] K.E. Gubbins, C.H. Twu, Chem. Eng. Sci. 33 (1978) 863.
[27] K.E. Gubbins, C.H. Twu, Chem. Eng. Sci. 33 (1978) 879.
[28] M. Luhmer, J. Reisse, J. Magn. Reson. Ser. A 115 (1995) 197.
[29] M. Luhmer, D. van Belle, J. Reisse, M. Odelius, J. Kowalewski, A. Laaksonen, J. Chem. Phys. 98 (1993) 1566.
[30] A. Dejaegere, M. Luhmer, M.L. Stien, J. Reisse, J. Magn. Reson. 91 (1991) 362.
[31] L. Sordelli, R. Psaro, G. Vlaic, A. Cepparo, S. Recchia, C. Dossi, A. Fusi, R. Zanoni, J. Catal. 182 (1999) 186.
[32] B. Bachiller-Baeza, A. Guerrero-Ruiz, P. Wang, I. Rodriguez-Ramos, J. Catal. 204 (2001) 450.
[33] P. Reyes, H. Rojas, G. Pecchi, J.C.G. Fierro, J. Mol. Catal. A Chem. 179 (2002) 293.
[34] S. Recchia, C. Dossi, N. Poli, A. Fusi, L. Sordelli, R. Psaro, J. Catal. 184 (1999) 1.
[35] T. Salmi, P. Maki-Arvela, E. Toukoniitty, A.K. Neyestanaki, L. Tiainen, L. Lindfors, R. Sjoholm, E. Laine, Appl. Catal. A Gen. 196 (2000) 93.
[36] A.M. Pak, D.V. Sokol'skii, S.R. Konuspaev, Kinet. Catal. 21 (1980) 491.
[37] Y. Izumi, Proc. Jpn. Acad. 53 (1977) 38.
[38] M. Boudart, AIChE J. 18 (1972) 465.
[39] J.J. Carberry, Chemical and Catalytic Engineering, McGraw–Hill, New York, 1976.
[40] C.N. Satterfield, Mass Transfer in Heterogeneous Catalysis, MIT Press, Cambridge, MA, 1970.
[41] A. Wheeler, Adv. Catal. 3 (1951) 250.
[42] R.R. Hudgins, Can. J. Chem. Eng. 50 (1972) 427.
[43] A. Chantong, F.E. Massoth, AIChE J. 29 (1983) 725.
[44] E. Velo, L. Puigjaner, F. Recasens, Ind. Eng. Chem. Res. 29 (1990) 1485.
[45] D.E. Mears, Ind. Eng. Chem. Process Des. Dev. 10 (1971) 541.
[46] P.B. Weisz, C.D. Prater, Adv. Catal. Relat. Subj. 6 (1954) 143.
[47] P.B. Weisz, Z. Phys. Chem. (Frankfurt am Main) 11 (1957) 1.
[48] R.R. Hudgins, Chem. Eng. Sci. 23 (1968) 93.
[49] E.E. Petersen, Chem. Eng. Sci. 20 (1965) 587.
[50] W.E. Steward, J.V. Villadsen, AIChE J. 15 (1969) 28.
[51] K.B. Bischoff, Chem. Eng. Sci. 22 (1967) 525.
[52] R.M. Koros, E.J. Nowak, Chem. Eng. Sci. 22 (1967) 470.
[53] M.A. Vannice, B. Sen, J. Catal. 115 (1989) 65.
[54] R. Touroude, J. Catal. 65 (1980) 110.
[55] A. Patil, M.A. Banares, X. Lei, T.P. Fehlner, E. Wolf, J. Catal. 159 (1996) 458.
[56] P. Gallezot, D. Richard, Catal. Rev. Sci. Eng. 40 (1998) 81.
[57] E.W. Thiele, Ind. Eng. Chem. 31 (1939) 916.
[58] R. Aris, Introduction to the Analysis of Chemical Reactors, Prentice–Hall, Englewood Cliffs, NJ, 1965.
[59] P.A. Ramachandran, R.V. Chaudhari, Three-Phase Catalytic Reactors, Gordon and Breach Science Publishers, New York, 1983.
[60] C.N. Satterfield, J.R. Katzer, Adv. Chem. Ser. 102 (1971) 193.
[61] B.D. Prasher, G.A. Gabrill, AIChE J. 24 (1978) 1118.
[62] C.N. Satterfield, C.K. Colton, W.H. Pitcher Jr., AIChE J. 19 (1973) 628.
[63] J.M. Smith, Chemical Engineering Kinetics, third ed., McGraw–Hill, New York, 1981.
[64] D.N. Miller, R.S. Kirk, AIChE J. 8 (1962) 183.
[65] N. Wakao, J.M. Smith, Chem. Eng. Sci. 17 (1962) 825.
[66] M. Ternan, Can. J. Chem. Eng. 65 (1987) 244.
[67] R.P. Danner, T.E. Daubert, Manual for Predicting Chemical Process Design Data, Design Institute for Physical Property Data, American Institute of Chemical Engineers, New York, 1983.
[68] C.R. Wilke, P. Chang, AIChE J. 1 (1955) 264.
[69] W. Hayduk, H. Laudie, AIChE J. 20 (1974) 611.
[70] C.J. King, L. Hsueh, K. Mao, J. Chem. Eng. Data 10 (1965) 348.

[71] C.S. Caldwell, A.L. Babb, J. Phys. Chem. 60 (1956) 51.
[72] J. Leffler, H.T. Cullinan, Ind. Eng. Chem. Fund. 9 (1970) 84.
[73] Y.P. Tang, D.M. Himmelblau, AIChE J. 11 (1965) 54.
[74] U.K. Singh, M.A. Vannice, Appl. Catal. A Gen. 213 (2001) 1.
[75] G.C.M. Colen, G. Van Duijn, H.J. Van Oosten, Appl. Catal. 43 (1988) 339.
[76] T.E. Daubert, R.P. Danner, Physical and Thermodynamic Properties of Pure Chemicals: Data Compilation, Hemisphere Pub. Corp., New York, 1989.
[77] A.L. Lydersen, Estimation of Critical Properties of Organic Compounds by the Method of Group Contributions, Univ. Wisc. Eng. Exp. Stn. Rep., vol. 3, 1955.
[78] C.F. Spencer, T.E. Daubert, AIChE J. 19 (1973) 482.
[79] C.F. Spencer, R.P. Danner, J. Chem. Eng. Data 17 (1972) 236.
[80] D. van Velzen, R.L. Cardozo, Ind. Eng. Chem. Fund. 11 (1972) 20.
[81] B.I. Lee, M.G. Kesler, AIChE J. 21 (1975) 510.
[82] J.H. Hildebrand, R.L. Scott, The Solubility of Nonelectrolytes, third ed., Am. Chem. Soc. Monograph Ser., vol. 17, Reinhold, New York, 1950.
[83] G. Soave, Chem. Eng. Sci. 27 (1972) 1197.
[84] J.M. Moysan, M.J. Huron, H. Paradowski, J. Vidal, Chem. Eng. Sci. 38 (1983) 1085.
[85] J.M. Prausnitz, R.N. Lichtenthaler, E.G. Azevedo, Molecular Thermodynamics of Fluid-Phase Equilibria, second ed., Prentice–Hall, Englewood Cliffs, NJ, 1986.
[86] L. Cerveny, V. Ruzicka, Catal. Rev. Sci. Eng. 24 (1982) 503.
[87] L. Cerveny, A. Prochazka, V. Ruzicka, Collect. Czech. Chem. Commun. 39 (1974) 2463.
[88] L. Cerveny, J. Mojzisova, V. Ruzicka, J. Chem. Tech. Biotechnol. A 35 (1985) 161.
[89] J. Hajek, D.Y. Murzin, Ind. Eng. Chem. Res. 43 (2004) 2030.
[90] C.L. Young, Hydrogen and Deuterium, Solubility Data Series, vol. 5/6, Pergamon Press, Oxford, NY, 1981.